CHAPTER IV
RESULTS AND DISCUSSION

Results of each test in characterization and catalyst activity testing are presented and discussed in this chapter. This chapter is organized as characterization with different techniques and steps of activity testing as mentioned in Chapter III. The outcomes of each characterization and activity measurement step are presented consecutively after the results.

4.1 Catalyst Characterization

In different steps i.e. catalyst preparation, activity testing and after activity testing, catalysts were characterized to obtain supportive information for evaluating preparation parameters and catalytic performance. Results of each characterization are presented in the following sections.

4.1.1 TG - DTG Analysis

Thermo gravimetric analysis was done prior to calcination of selected catalysts for the purpose of determining the precursor salt decomposition temperatures. The test was carried out with TGA instrument in N_2 and O_2 environment, which is almost equivalent to the composition of air (79 % N_2 and 21 % O_2). The temperature program from room temperature to 700 °C was used with a heating rate of 10 °C/min.

TG - DTG results for Fe/KL zeolite and FePt/KL zeolite catalysts are presented in Figure 4.1. As shown, the presence of Pt in Fe/KL zeolite promotes the Fe precursor decomposition. Fe/KL zeolite shows significant weight loss up to 500 °C, suggesting that calcination after IWI has to be performed at 500 °C or above. The FePt/KL exhibits much lower decomposition temperature as complete weight loss was observed at 350 °C. Even though it shows a decrease in decomposition temperature, 500 °C was used as calcining temperature for both types of catalysts.

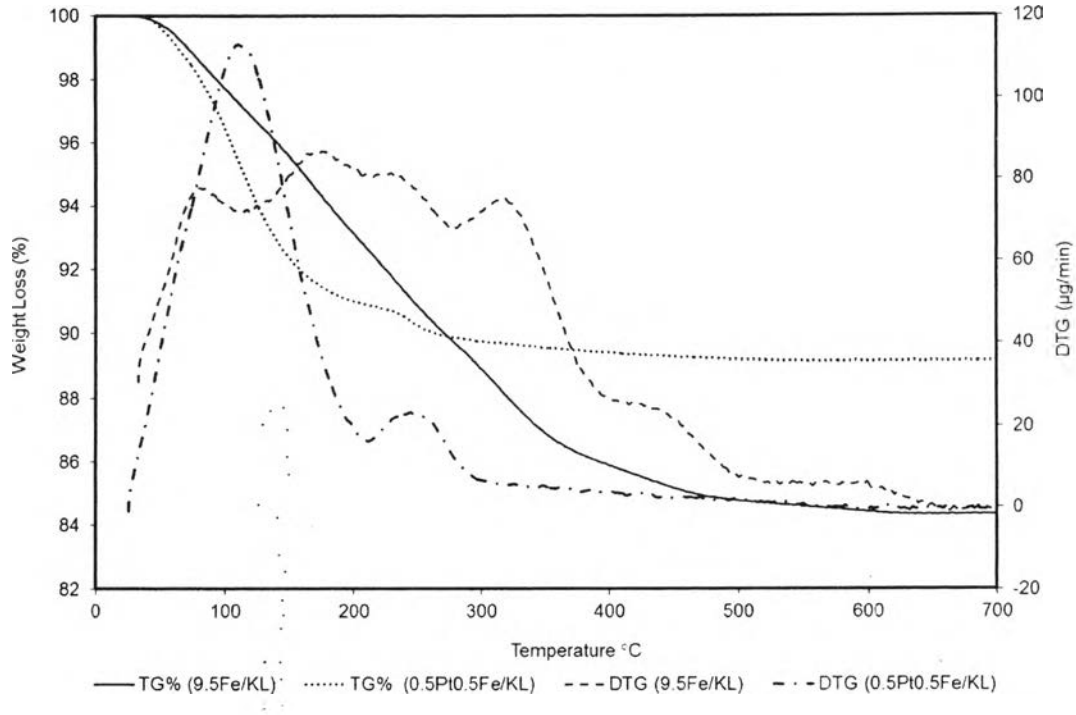

Figure 4.1 TG-DTG results for Fe/KL and FePt/KL catalysts.

4.1.2 Temperature Programmed Reduction (TPR)

A series of TPR tests were carried out for different catalysts in order to observe the reducibility of each metal species in the catalyst. TPR tests were carried out with micrometric temperature programmed reduction (TPR) apparatus equipped with TCD by using H_2 (10 cm^3/min for around 50 mg of each catalyst) as reducing agent and temperatures 30 °C to 800 °C. Pt/KL, Fe/KL, FePt/KL and physically mixed Fe/KL and Pt/KL catalysts were tested. The results are presented in Figure 4.2.

According to the TPR analysis it shows that Fe oxide on KL zeolite was reduced giving three peaks at 420, 600, and 800 °C which suggest that the reduction follow through Fe_2O_3 Fe_3O_4, FeO to α-Fe as shown in Figure 4.2 (Zilinski *et al.*, 2010). Here in this case, the temperature was increased with the rate of 10 °C/min and hence peaks have been moved to higher temperatures. The temperature of 400 °C was used as the reduction temperature as used in most of the literature with Fe based catalysts with almost all the supports.

In addition, in the case of 0.5Pt/KL catalysts, two key peaks were observed around 280 and 400 °C, which could be related to Pt^{+} and Pt^{2+}. Further, in the case of FePt/KL, only three key peaks were observed around 200, 350, and 600 °C, which could be mainly related to Fe, and peaks related to Pt could be overlapped with new Fe peaks. The peak locations have been shifted to lower temperatures and this could be due to the promotion on reduction of Fe species by the available Pt sites.

In the case of physically mixed catalysts, a shift of peaks to lower temperatures was observed but the shift is lower than the case of co-impregnation. This behavior could be due to the unavailability of Pt and Fe in the same or much closer sites. In both the cases it can be concluded that the available Pt promote the reduction of Fe species.

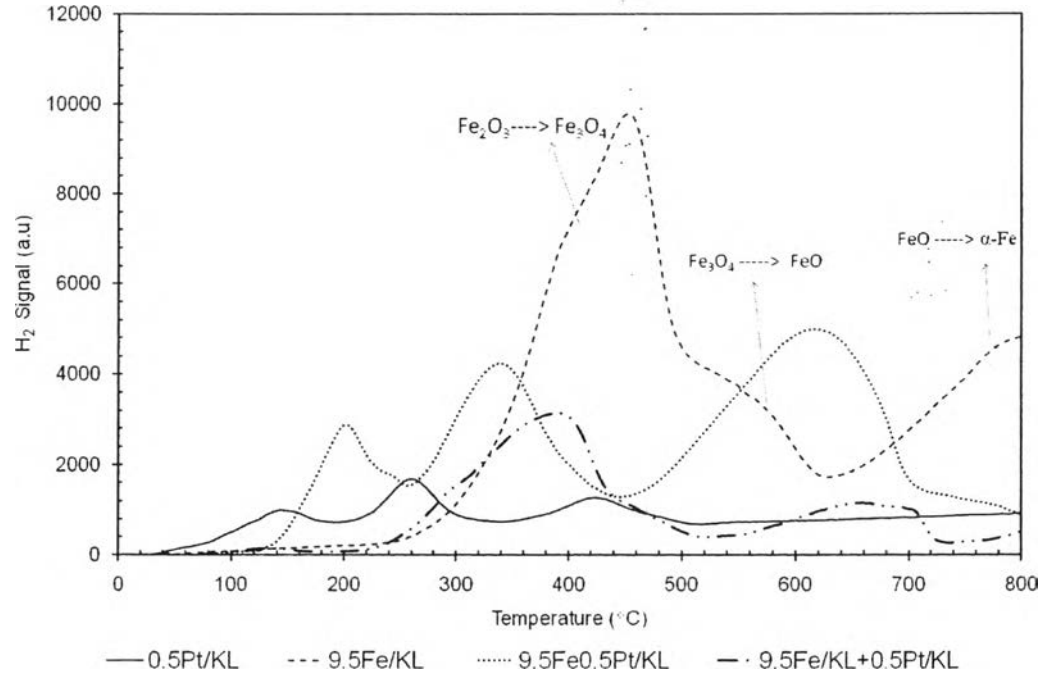

Figure 4.2 TPR results for Fe and Pt based catalysts supported on KL zeolite.

4.1.3 Nitrogen Adsorption/Desorption Analysis

Nitrogen adsorption/desorption was carried out in order to determine the surface area and pore volume of catalysts by using microspore analysis. Quantachrome Autosorb 1MP instrument was used for analysis. As in the procedure for the instrument, sample tube was outgassed at 150 °C and the catalyst samples were outgassed at 300 °C for more than 8 h prior to the N_2 adsorption at liquid N_2 temperature.

KL zeolite, 0.5Pt/KL and 9.5Fe/KL were tested to observe the influence of Fe or Pt addition on pore volume. BET surface area and pore volume data were observed to determine the influence of metal addition on pore blockage. BET surface area analysis for FeCoK catalyst was also conducted to observe the surface area. The results for KL zeolite, 9.5Fe/KL, 0.5Pt/KL, and FeCoK can be presented as in Table 4.1.

Table 4.1 BET measurement results of KL support, 9.5Fe/KL, 0.5Pt/KL and FeCoK catalysts

Catalyst	BET Surface area (cm^2/g)	Total Pore volume (cm^3/g)	Cumulative pore vol. SF (cm^3/g)	Cumulative pore vol. DFT (cm^3/g)
KL support	389.2	0.3756	0.1998	0.2284
9.5Fe/KL	46.29	0.2096	0.0214	0.0748
0.5Pt/KL	270.9	0.2838	0.1390	0.1613
FeCoK	36.44	--	--	--

As indicated in Table 4.1, the surface area of KL zeolite is drastically dropped with impregnation of 9.5 percent of Fe on it, giving an evidence of blocking the pores, which mainly contribute to the surface area of zeolite. In addition, the increase in the average pore diameter indicates that only larger pores remained unblocked when 9.5% of Fe in the catalyst. In the case of 0.5% of Pt addition, it was observed that significant portion of pores is available unblocked. The plot between pore width and cumulative surface area and pore volume (NLDFT) clearly indicates that pores having diameter less than 0.85 nm (0.65-0.85 nm) govern the major

portion of KL zeolite surface area and the pore volume. As indicated in Figure 4.3, the contribution from pores having diameter of less than 0.85 nm is drastically reduced in the case of 9.5Fe/KL catalyst providing further evidence of pore blockage. 0.5Pt/KL seems carrying significant amount of unblocked pores.

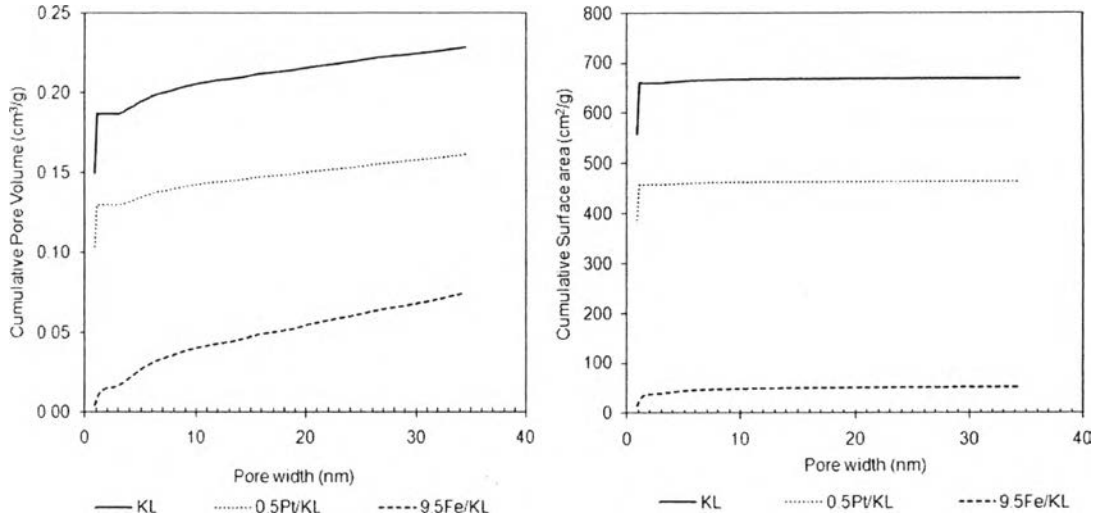

Figure 4.3 N_2 adsorption/desorption results (a) Cumulative pore volume (NLDFT) with pore width; (b) Cumulative surface area (NLDFT) with pore width.

N_2 adsorption/desorption analysis for FeCoK catalyst was also conducted to check whether the surface area of catalyst is sufficient for effective FT synthesis. In the surface area analysis for the calcined FeCoK catalyst with Quantacrome Autosorb 1MP instrument, the surface area of the catalyst was observed as 36.44 m^2/g as shown in Table 4.1. This information gives evidence that FeCoK catalyst satisfies the requirement of surface area for FT synthesis.

The surface area of FeCoK catalysts should be greater than 5 m^2/g for calcined state to obtain better performance for production of hydrocarbon containing C_2-C_{20} olefins in FT synthesis (Soled *et al.*, 1985).

4.1.4 X-Ray Diffraction (XRD)

XRD analysis was carried out for different catalysts to observe the crystalline form of each catalyst. XRD analysis was conducted before and after the activity testing to observe the formation of carbide phases in the reaction and to

observe the form of oxide present after calcination. In addition, another objective of this analysis was to observe the presence of unreduced oxides after the reaction which can be affected to the variations in the activity of different catalysts.

The XRD analysis for Fe/KL and FeCoK catalysts before and after reaction was conducted from 2θ of 10.0° to 80.0° with 0.02° steps with D8 advance x-ray diffraction instrument and the profiles are presented in Figures 4.3 and 4.4.

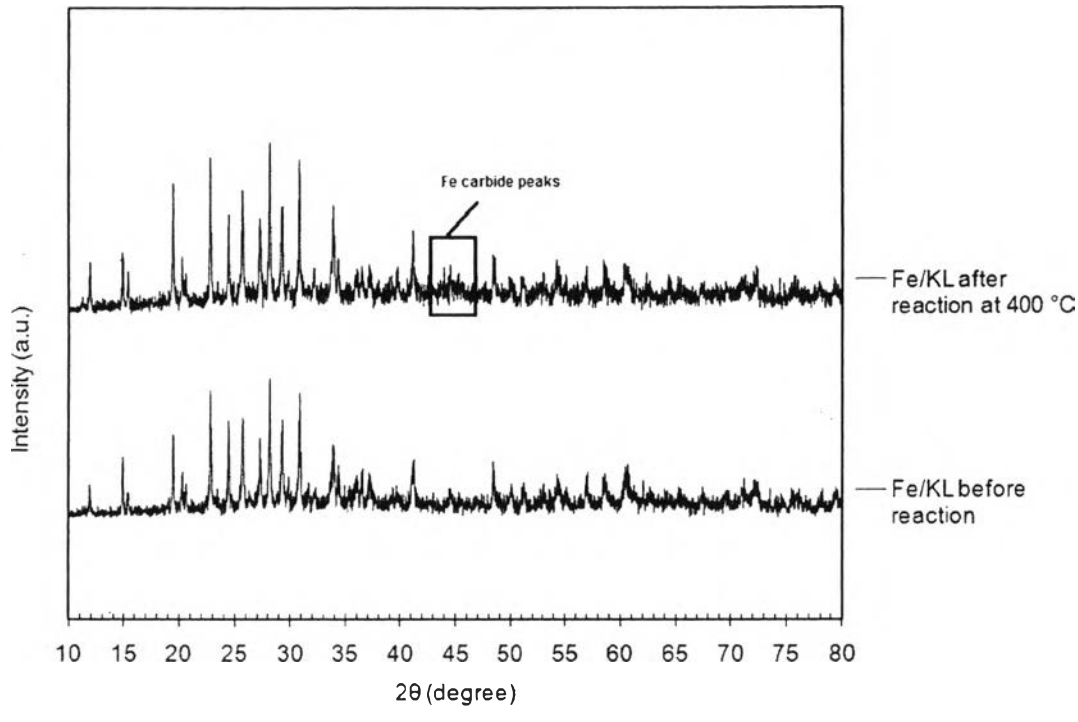

Figure 4.4 XRD profiles of Fe/KL catalysts before and after reaction.

With the analysis, it is clear that the main component in calcined catalysts is hematite (Fe_2O_3) and in the same catalyst after reaction at 400 °C shows the presence of iron carbide phases mainly χ-carbide (Fe_5C_2) after reaction. It is a mixture of species which are not most active for FT synthesis.

According to the XRD profiles presented in Figure 4.5 for FeCoK catalyst, it is observed that the calcination temperature in the second step (after K impregnation) has no significant impact on the form of iron oxides presence showing equal pattern of XRD profiles. In the case of after the reaction, the oxide phases disappeared while new phases emerge. The new phases emerged consist of different carbides as Fe_5C_2 and Fe_7C_3 together with α-Fe which is good combination for FT

activity as concluded by Linde D. and his co-workers. This could be identified as the reason for better FT activity of FeCoK catalyst compared to Fe/KL. Magnetite is also present in the spent catalyst, which may be due to poor preserving of the sample before XRD analysis.

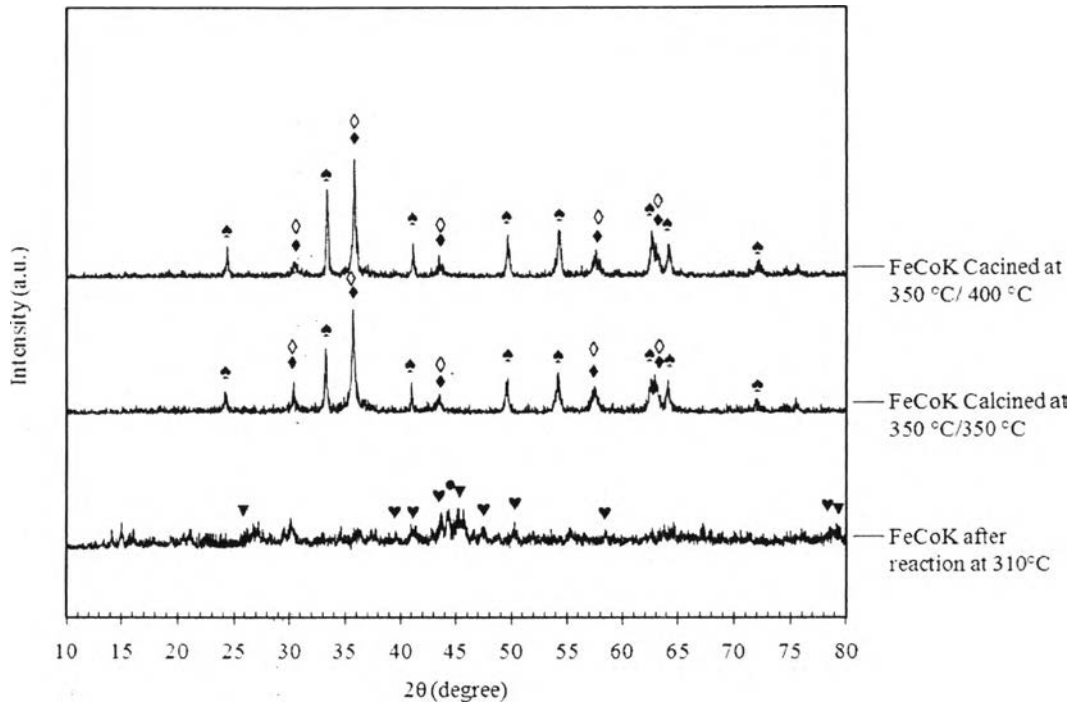

Figure 4.5 XRD profiles for FeCoK catalysts with different calcinations temperatures and after reaction at 310 °C (♠) Fe_2O_3 (◊) Fe_3O_4 (♦) $CoFeO_4$ (♥) Fe_7C_3 (▼) Fe_5C_2 (●) α-Fe.

4.1.5 Temperature Programmed Oxidation (TPO)

TPO tests were carried out to determine the amount and properties of coke formed in the reaction. All spent catalysts were analyzed by using the instrument, which consists of a methanator to convert CO_2 produced to methane and an online FID to detect it. Coke deposited on the catalyst was burnt with 2% O_2 in He.

TPO analysis was carried out for different series of catalysts and the profiles were plotted in separate graphs depending on the requirement of analysis. Fe/KL zeolite were tested for FT activity at different temperatures and the TPO profiles for three different temperatures is presented in Figure 4.6 and total carbon

content in each catalyst is presented in Table 4.2. According to the results it can be observed that the coke deposited on catalysts after reaction at 240 °C and 300 °C are burnt at around 375 °C while the burning of coke for reaction at 400 °C appears around 525 °C. This gives evidence of forming different types of coke by FT synthesis at 400 °C.

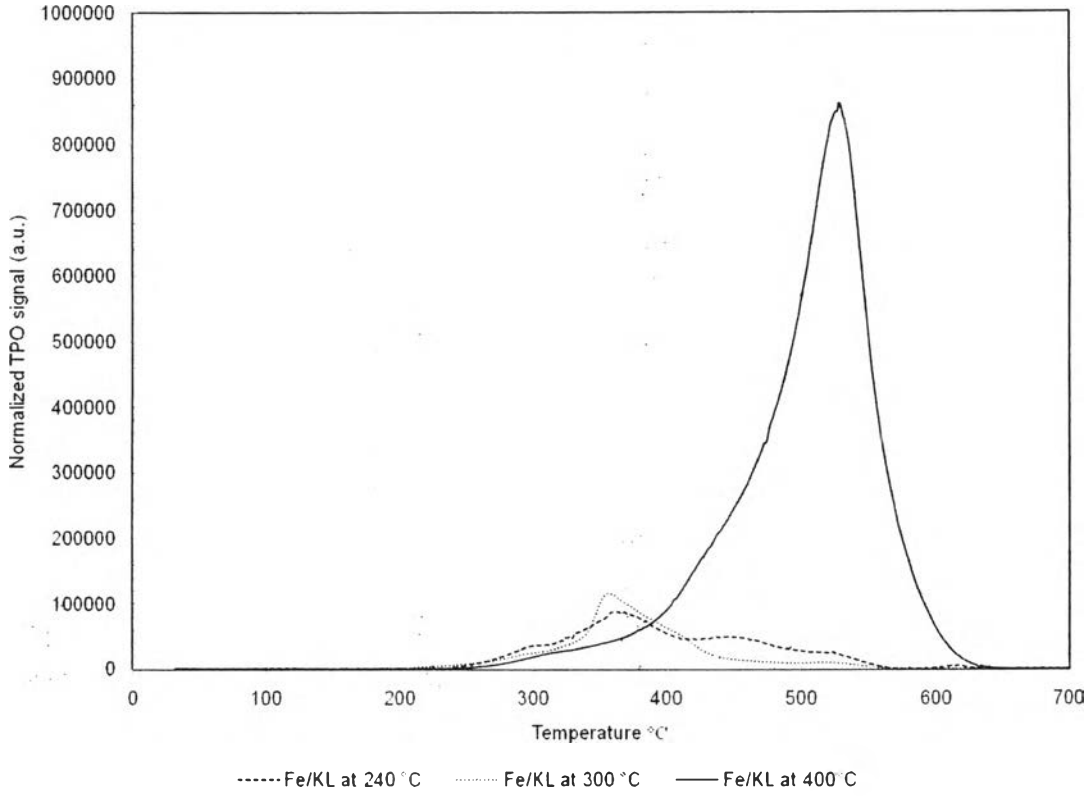

Figure 4.6 TPO profiles for Fe/KL zeolite catalysts after FT reaction at different temperatures (P = 1 atm, GHSV = 6,000 $cm^3/g.h$, H_2/CO = 1.5).

Table 4.2 C content in spent 9.5Fe/KL catalysts after FT reaction at 240, 300 and 400 °C (TOS = 360 min, P = 1 atm, GHSV = 6,000 $cm^3/g.h$, H_2/CO = 1.5)

Reaction temperature (°C)	C content in spent catalyst (wt. %)
240	3.62
300	4.56
400	25.19

Based on the C content in catalyst from TPO analysis, it is observed that C content in catalyst is increased with increasing reaction temperature. This is also in line with high CO_2 production at high temperature which can be produced by Boundard reaction ($2CO \rightarrow CO_2 + C$).

TPO profiles of co-impregnated 9.5Fe0.5Pt/KL catalyst and 9.5Fe/KL physically mixed with 0.5Pt/KL after syngas aromatization at 400 °C and Fe/KL catalyst after FT synthesis at 400 °C are presented in Figure 4.7. It can be observed that the same form of coke is formed in both 9.5Fe/KL and physically mixed catalyst, which is burnt above 500 °C while another type of coke is formed on 9.5Fe0.5Pt/KL co-impregnated catalyst, which is burnt below 400 °C. In addition, it can be observed that slight reduction of C burning temperature for physically mixed catalyst than pure 9.5Fe/KL suggesting that available Pt has given some promotional effect on C oxidation. The lower temperature of C burning for co-impregnated catalyst can also be due to the reason of promotion from available Pt closer to Fe sites.

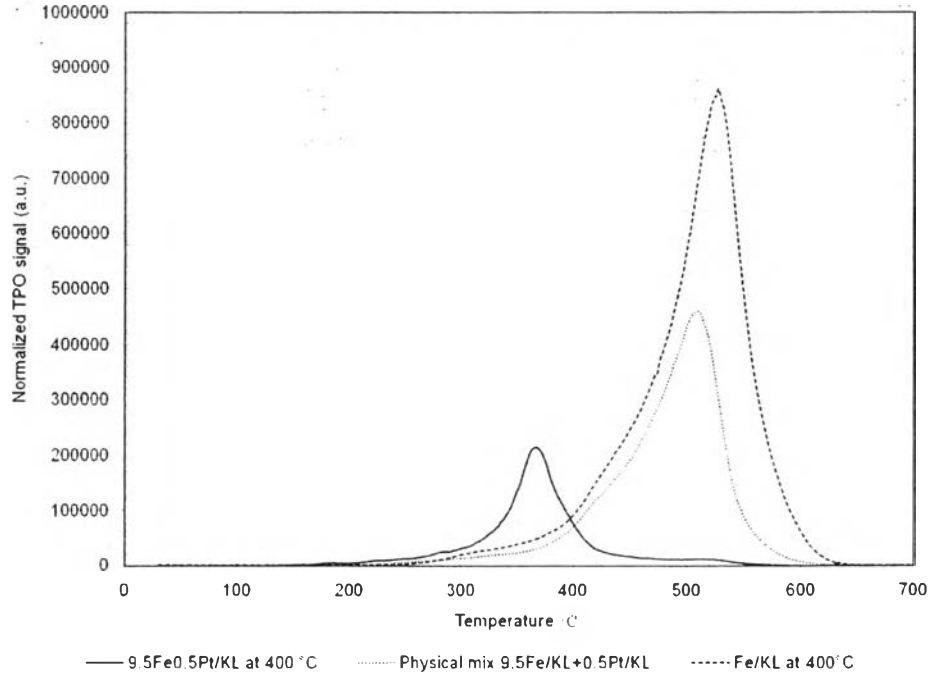

Figure 4.7 TPO profiles for co-impregnated, physically mixed and pure FT catalyst after reaction at 400 °C (TOS = 360 min, P = 1 atm, GHSV = 6.000 $cm^3/g.h$, H_2/CO = 1.5).

According to the calculations of C content, it can be observed that coke formation is the highest for 9.5Fe/KL catalyst with 25.19 wt.% of C while physically mixed and co-impregnated catalysts showed lower C content having 13.27 and 5.48 wt.% respectively as presented in Table 4.3.

Table 4.3 C content in spent after catalysts after FT and aromatization reactions at 400 °C (TOS = 360 min, P = 1 atm, GHSV = 6,000 cm^3/g.h, H_2/CO = 1.5)

Catalyst	C content in spent catalyst (wt. %)
9.5Fe/KL (impregnated)	25.19
9.5Fe/KL+0.5Pt/KL (physical mix)	13.27
9.5Fe0.5Pt/KL (co-impregnated)	5.48

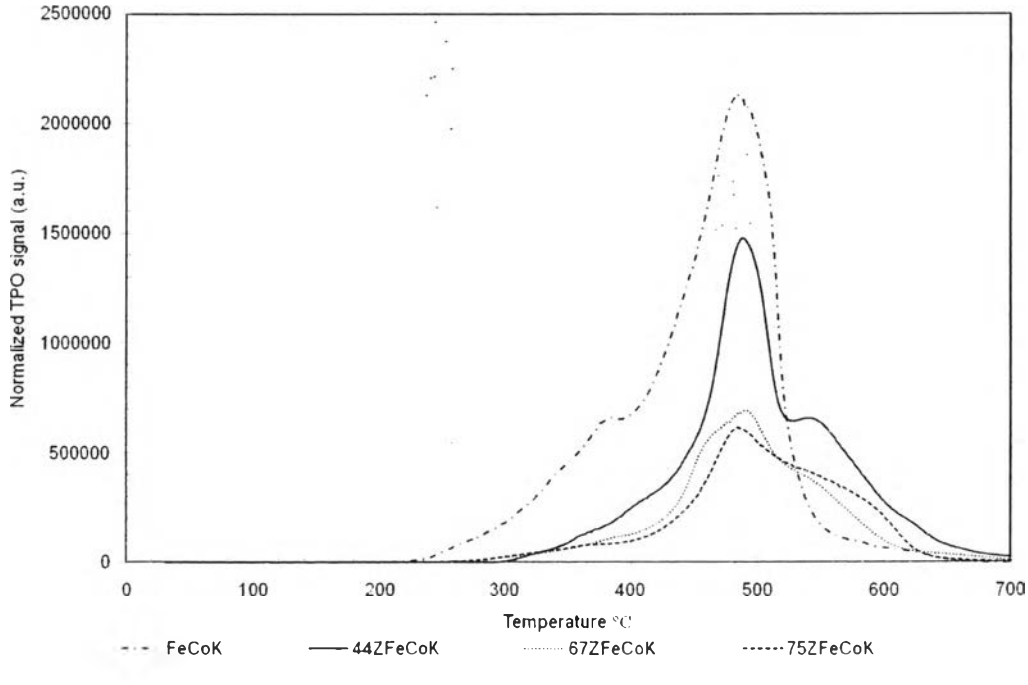

Figure 4.8 TPO profiles for FeCoK after FT reaction and physically mixed FeCoK and HZSM5 hybrid catalysts after syngas aromatization reaction at 310 °C (P = 20bar, GHSV = 4,800 cm^3/g.h, H_2/CO = 1.5, and TOS = 430 min).

Further, series of TPO tests were conducted for physically mixed FeCoK and HZSM5 hybrid catalysts, which contains different amount of HZSM5. According to the profiles which are presented in Figure 4.8, it is observed that it has more than one type of coke in catalyst when it combined with HZSM5. The shoulder in the right tail of the peak, which lies around 550 °C is providing evidence for this. It can be concluded that the peak below 500 °C should be related to FeCoK catalyst and the shoulder should be related to the HZSM5 aromatization catalyst.

Table 4.4 C content in spent catalysts after FT and aromatization reactions at 310 °C (TOS = 430 min, P = 20 bar, GHSV = 4,800 $cm^3/g.h$, H_2/CO = 1.5)

Catalyst	C content in spent catalyst (wt. %)
FeCoK	86.58
Hybrid catalyst (44ZFeCoK)	51.91
Hybrid catalyst (66ZFeCoK)	31.74
Hybrid catalyst (75ZFeCoK)	23.54

The C calculation in Table 4.4 showed a decrease in C content when the HZSM5 increases suggesting that coke formation is mainly in the FT catslyst. The decrease of C is due to the dilution of spent FeCoK catalyst with HZSM5 in the physical mixture.

4.1.6 Scanning Electron Microscopy with Energy Dispersive X-ray (SEM-EDX)

Scaning electron microscopy is used to observe the morphology of the catalysts. It was specially conducted for FeCoK catalyst to observe the surface behavior because it was synthesized by CP technique. SEM-EDX also conducted to observe the metal contents of the catalyst around the surface and to map the metal distribution with Hitachi/S-4,800 instrument. SEM images for FeCoK are presented in Figure 4.9 with different magnifications.

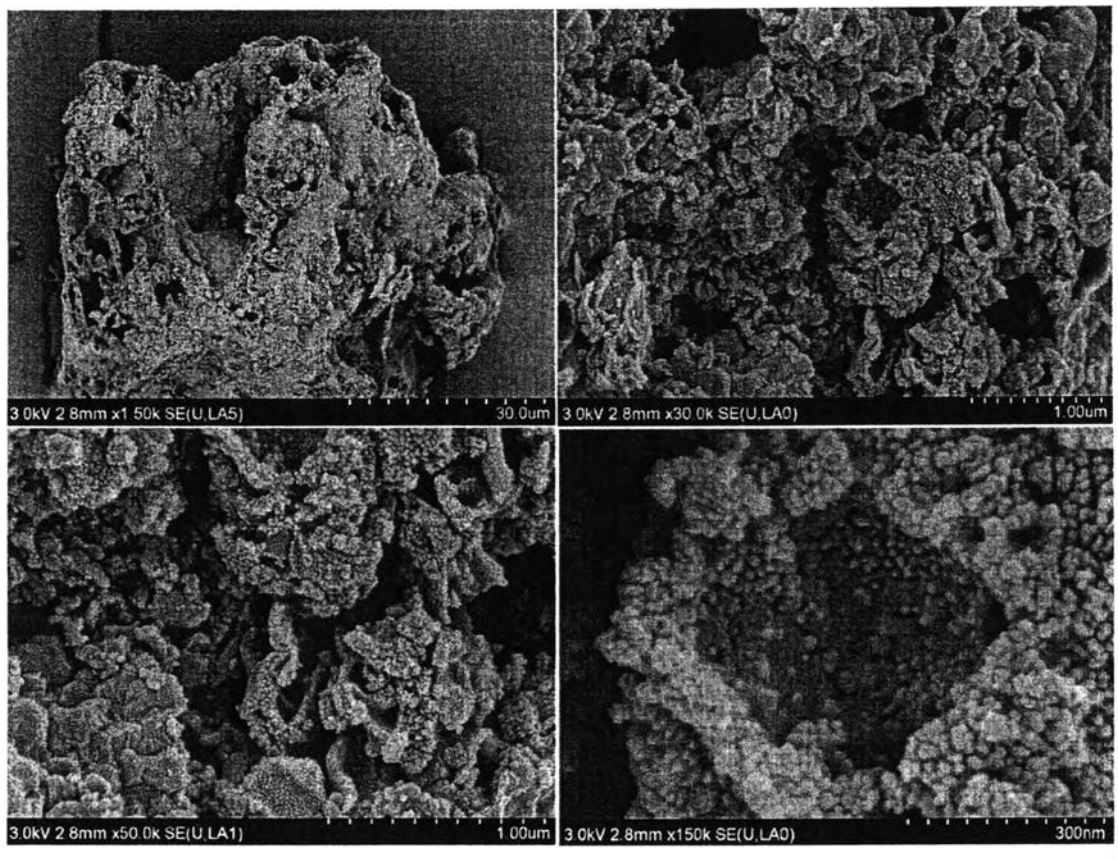

Figure 4.9 SEM images of FeCoK catalyst synthesized by co-precipitation technique with glycolic acid to form high surface area with calcinations at 350 °C and calcined 400 °C after K impregnation.

With the images, it can be observed that the catalyst is highly porous which give sufficient surface area for FT reaction. This is in line with the better surface area of 36.44 cm^2/g obtained in BET is greater than 5 cm^2/g, which is required for significant FT reaction activity (Soled *et al.*, 1985)

Elemental mapping from SEM-EDX and composition analysis at different locations of the FeCoK catalyst was conducted to estimate the composition and the distribution of metals throughout the catalyst. The elemental mapping images and composition data are presented in Figure 4.10 and Table 4.5.

It is clear from elemental mapping images that the metal content is decreased from Fe, Co to K. In addition, the all three elements are well distributed in the catalyst over the area of scan.

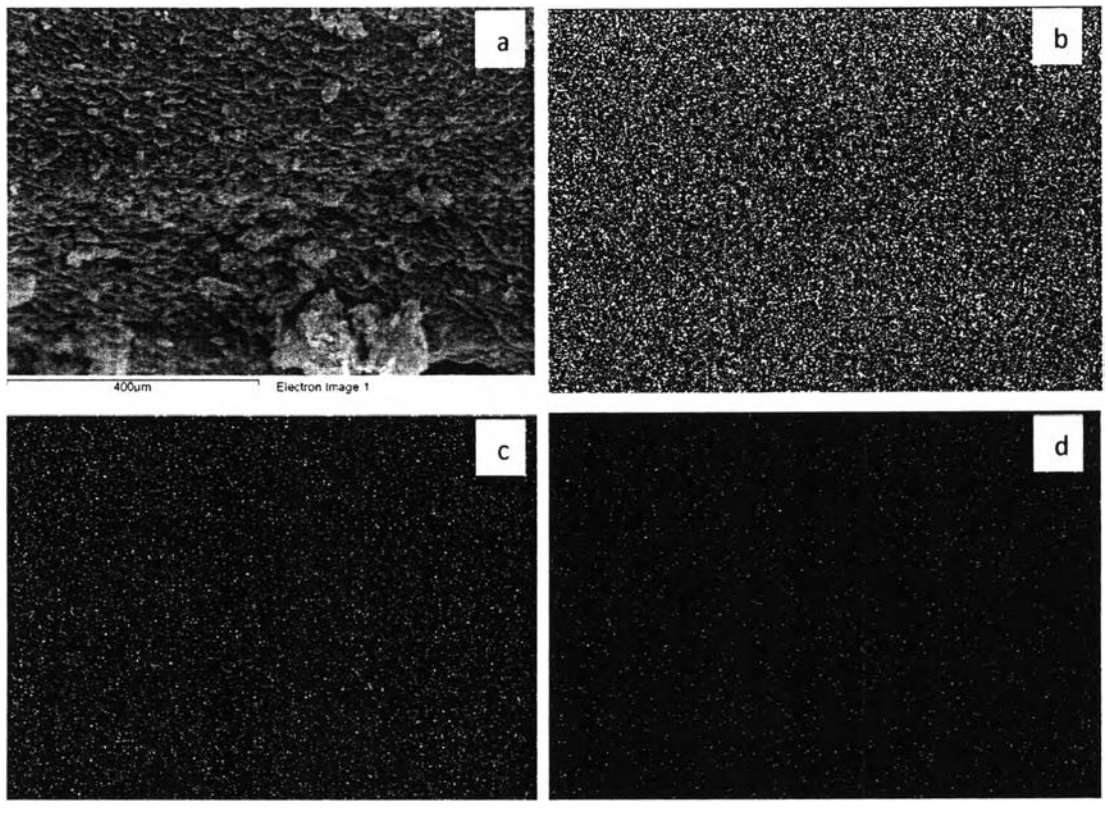

Figure 4.10 Elemental mapping images for FeCoK catalyst (a) Electron image of the location, (b) Fe distribution in the area of location in (a), (c) Co distribution in the area of location in (a), and (d) K distribution in the area of location in (a).

Table 4.5 Composition of the FeCoK catalyst determined by SEM-EDX technique measured at different locations of the catalyst

Element	Weight %			
	Location 1	Location 2	Average	Expected
Fe	94.33	95.70	95.02	92.08
Co	5.44	2.99	4.22	6.48
K	0.23	1.31	0.77	1.43
Total	100	100	100	100

Compositions determined in two (on two different particles) locations are presented in Table 4.5 and it shows that there are slight changes of composition in different locations. The catalysts were prepared with the expected weight percentage of 92.08, 6.48, and 1.43 for Fe, Co, and K respectively. The average

composition of the catalyst shows a higher percentage of Fe while having lower Co and K. This may be due to the error in determining low concentrations using SEM-EDX and the possible percentage errors in catalyst preparation step due to the lower metal additions.

4.2 Catalytic Activity Testing

Catalyst activity testing in this research is conducted in several steps as previously mentioned in the Chapter III. Activity testing was divided into steps depending on what are the requirements to ascertain in each step. Each step in catalytic activity testing is discussed here in detail with results.

4.2.1 Fischer-Tropsch Activity of Fe/KL Zeolite and FeCoK Catalysts

The catalytic activity testing in this step is mainly focused on deciding a temperature for aromatization of syngas and hence the reaction was carried out at different temperatures. Pt/KL zeolite is well-known for aromatization of hexane, heptane and octane. The product distribution from FT catalyst is expected to be in the range of range of hexane to octane for aromatization over Pt/KL.

9.5Fe/KL catalyst was tested for FT activity and product selectivity at three different temperatures i.e. 240, 350, and 400 °C. Other parameters were maintained as GHSV = 6,000 $cm^3/g.h$ (amount of catalysts used was 0.5 g and hence the actual feed flow rate was 50 cm^3/min), P = 1 atm, $H_2/CO = 1.5$.

The catalyst was packed as described in Chapter III and before the reaction catalysts were reduced at 400 °C for 3 h in situ with 100 cm^3/g of H_2. Then the rector temperature was adjusted to the reaction temperature and feed was introduced when the reaction temperature is reached. First sample analysis was conducted after 20 min from feed starts and then sampling was continued every hour except in the case of 400 °C and 300 °C which was every 110 minites.

Actually, this was carried out without any pre-carbiding after reduction of catalysts as mentioned in the work for FeCoK catalysts which was conducted to produce high octane gasoline from syngas (Martinez *et al.*, 2005).

In addition, another test was carried out to observe the activity and the product selectivity of FeCoK catalyst for FT reaction at 400 °C with reduction for 10

h with H_2 followed by carbiding with a mixture of $CO:H_2:He$ at 10:15:75 with a heating rate of 1 °C/min and maintained at 400 °C for 3h.

The conversion results from the above series of tests are illustrated as in Figure 4.11.

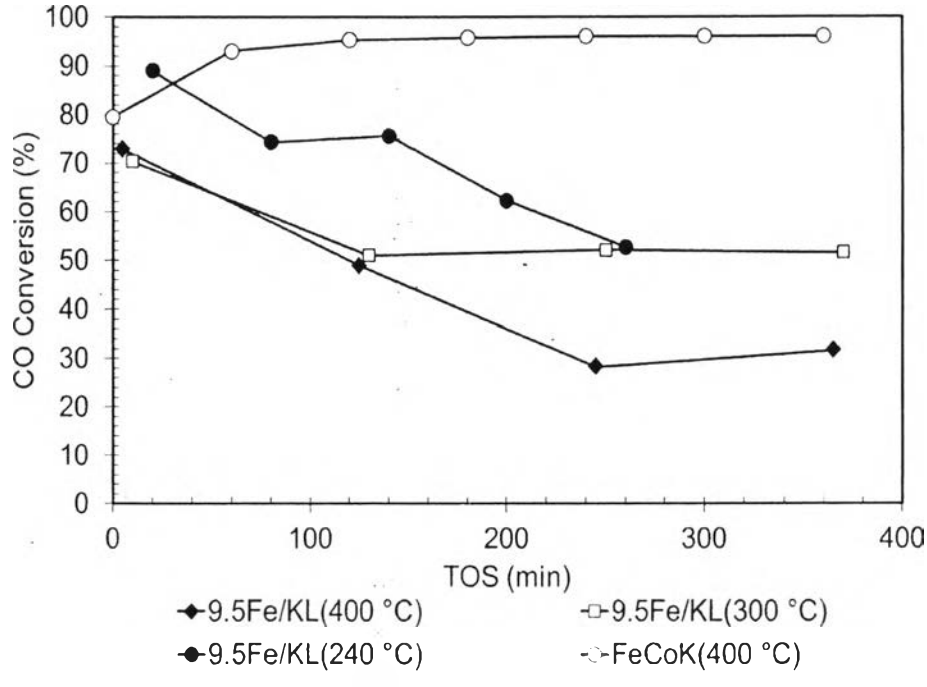

Figure 4.11 CO conversion change with operating temperature and catalyst type (GHSV = 6,000 $cm^3/g.h$, P = 1 atm and H_2/CO = 1.5).

The results show that the conversion of CO decreased with time on stream with 9.5Fe/KL catalyst. On the other hand, FeCoK catalyst maintained a stable activity over time. In addition, for 9.5Fe/KL catalysts, the conversion at a given time on steam is decreased with temperature increased from 240 °C to 400 °C upto 280 min TOS. In the conversion point of view, 240 °C is better than other two temperatures among 9.5Fe/KL catalysts but FeCoK catalysts shows much higher conversion for all values of time on stream.

In Figures 4.12 - 4.15, the product selectivity of CO_2, CH_4 and C_{3+} fraction are illustrated.

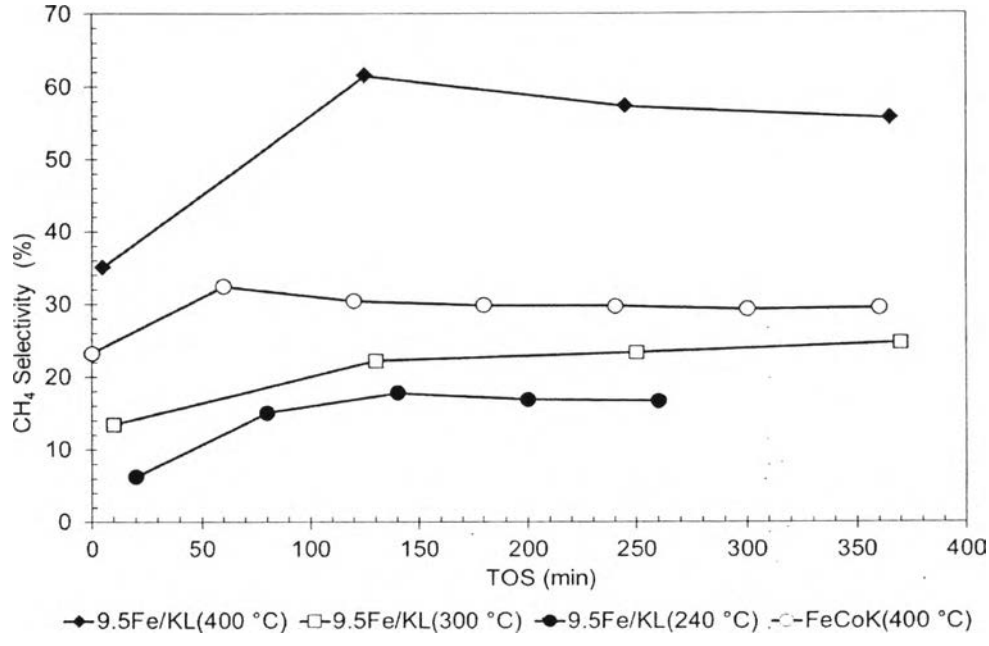

Figure 4.12 CH_4 selectivity change with operating temperature and catalyst type (GHSV = 6,000 cm^3/g.h, P = 1 atm and H_2/CO = 1.5).

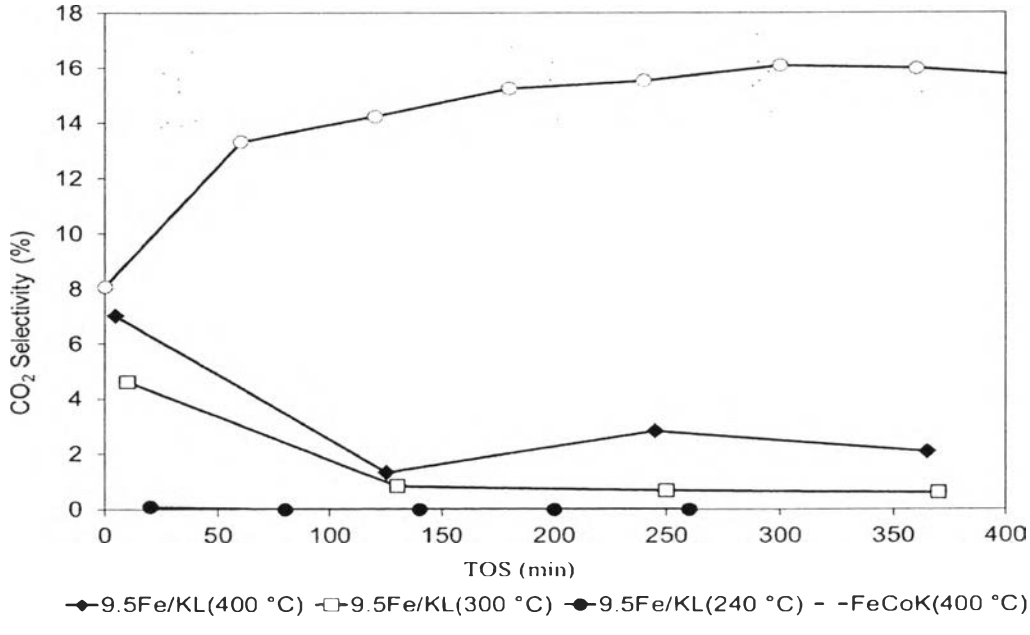

Figure 4.13 CO_2 selectivity change with operating temperature and catalyst type (GHSV = 6,000 cm^3/g.h, P = 1 atm and H_2/CO = 1.5).

It can be observed that the selectivity to CH_4 and CO_2 is significantly influenced by temperature for Fe/KL catalysts. Those products are lower value,

highly stable products, which can hardly follow further reaction without extreme conditions. Moreover, at the same temperature, FeCoK catalysts produce much less CH_4 compared to Fe/KL but higher CO_2 selectivity. Even though CO_2 selectivity is higher with FeCoK catalyst, the combined selectivity of CH_4 and CO_2 is higher in 9.5Fe/KL zeolite catalyst for the reaction at same conditions giving better performance with FeCoK catalyst having lower selectivity to undesirable products.

As previously discussed in TPO analysis in Figure 4.6 and Table 4.2, it shows that the amount of C in the spent catalyst is increased with increasing temperature and the results of CO_2 production is also in line with the C results. These interrelated results can suggest that the C and CO_2 is produced by Boundard reaction ($2CO \rightarrow C+CO_2$).

In this work, it is expected to have hydrocarbons with higher carbon number, which can follow through aromatization with Pt/KL zeolite catalysts, hence lower methane selectivity is better for future work in aromatization. It was observed that the C_{3+} hydrocarbon fraction was decreased with increasing reaction temperature for Fe/KL zeolite catalysts leading to negligible C_{3+} fraction at 400 °C. In contrast, FeCoK catalyst showed a significant selectivity towards C_{3+} at higher temperatures as 400 °C giving around 18% as presented in Figure 4.14. Even though the C_{3+} fraction was higher in the cases of 9.5Fe/KL at 300 °C and 240 °C, the temperatures are too low for aromatization with Pt/KL. Hence, FeCoK was selected as the best candidate with significant selectivity to C_{3+} at reasonably higher temperature (400 °C) to study about aromatization with Pt/KL catalyst.

Olefins in the products also have a significant influence on aromatization depending on the mechanism. If the mechanism follows through oligomerization followed by aromatization, the presence of olefins is favored than paraffins (Martinez *et al.*, 2005). As illustrated in Figure 4.15, higher olefin products were observed with Fe/KL catalysts at all the tested temperatures compared to FeCoK catalyst.

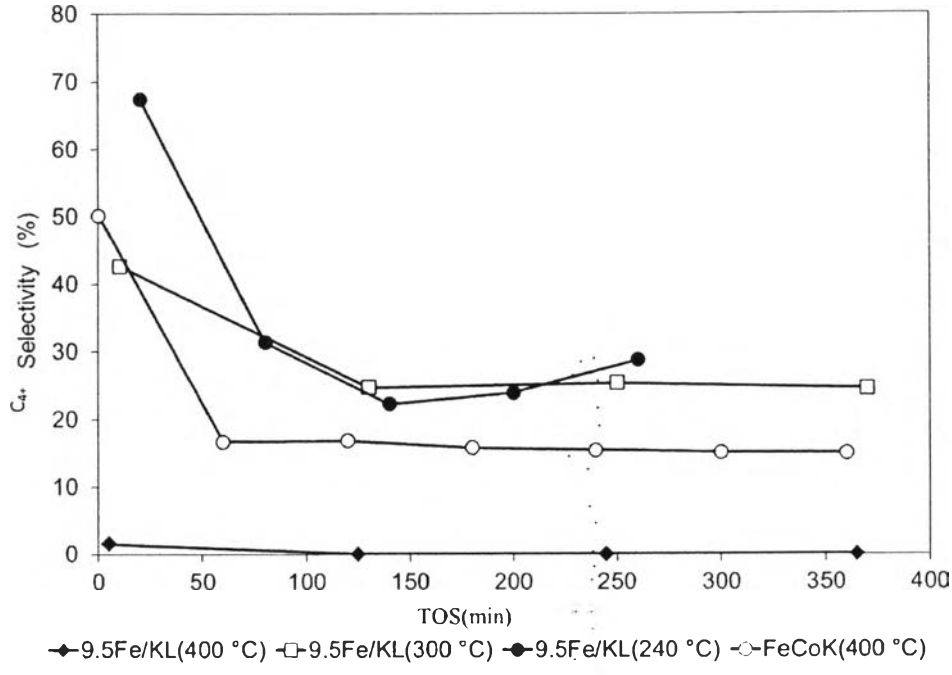

Figure 4.14 C_{4+} fraction change with operating temperature and catalyst type (GHSV = 6,000 cm^3/g.h, P = 1 atm and H_2/CO = 1.5).

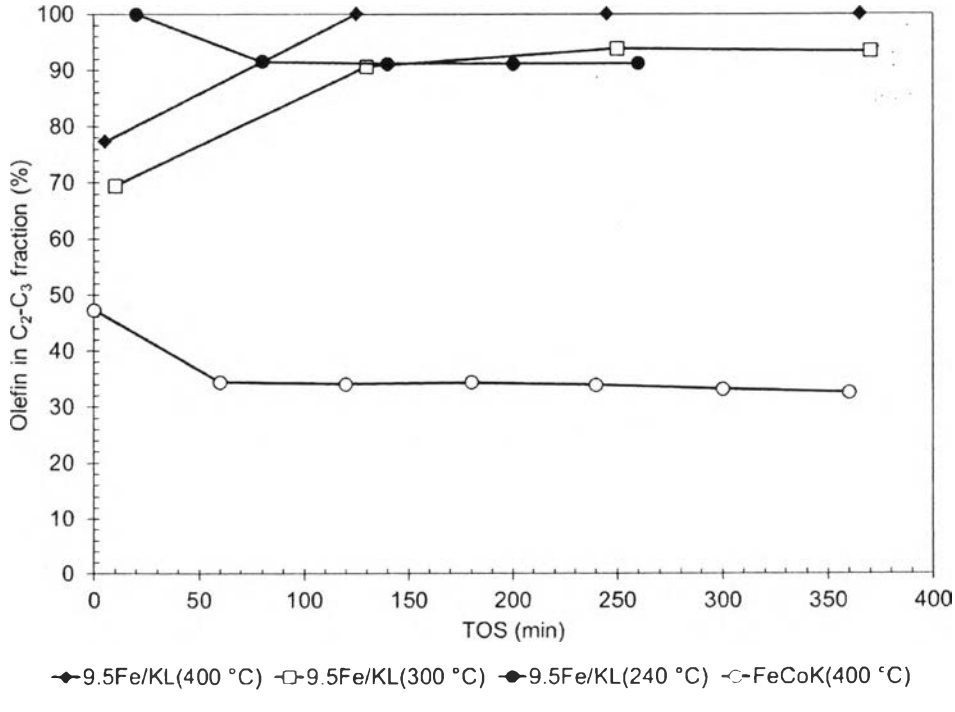

Figure 4.15 Percentage of olefin in C_2-C_3 fraction for different temperatures and catalysts types (GHSV = 6,000 cm^3/g.h, P = 1 atm and H_2/CO = 1.5).

Total products obtained from reactions at different reaction temperatures after around 250 min TOS are presented in Table 4.6 with their respective carbon number.

Table 4.6 Conversion and product selectivity for FT synthesis at different temperatures with different catalyst type

Conversion/Selectivity	9.5Fe/KL			FeCoK
	240 °C	300 °C	400 °C	400 °C
CO Conversion	52.67	52.10	28.21	96.06
Product selectivities				
CO_2	0.00	0.69	2.83	15.55
C_1	16.66	23.34	57.31	29.74
C_2	31.63	27.43	24.37	11.64
C_3	18.75	22.49	12.66	12.06
C_{4-}	28.71	25.35	0.00	15.46

4.2.2 Syngas Aromatization with Co-impregnated FePt/KL and Physically Mixed Catalysts

Aromatization of syngas was conducted with combined catalysts for FT synthesis and aromatization. Co-impregnated 9.5Fe0.5Pt/KL zeolite catalyst was used to obtain the FT activity from Fe sites and aromatization by Pt sites. Physical mixture of 9.5Fe/KL zeolite and 0.5Pt/KL zeolite, which contain the same amount of active metal, was also tested with same conditions. The feed gas rate was maintained to obtain the same GHSV relative to FT catalyst only.

The conditions for the reaction was maintained at GHSV = 6,000 $cm^3/g.h$, P = 1 atm, T = 400 °C and H_2/CO = 1.5 for both co-impregnated and physically mixed catalysts. The conversion and product selectivity are presented in Figures 4.16 – 4.22.

As shown in Figure 4.16, the conversion is slightly lower for physically mixed catalyst compared to co-impregnated catalyst having around 55 %

and 65 % respectively at initial stages. This could be due to lower coke formation in co-impregnated catalysts as in detected in TPO results presented in Figure 4.7 and Table 4.2. Further, with information in Figure 4.17, the methane selectivity is more than twice for physically mixed catalyst compared to co-impregnated showing around 70 % after 200 min on steam. The CO_2 selectivity has no significant difference between two catalysts.

The higher CH_4 selectivity in physically mixed catalyst may be due to the more accessible Pt sites in 0.5Pt/KL catalyst. The Pt sites in 9.5Fe0.5Pt/KL catalyst could be inaccessible due to the pore blockage as observed in BET analysis in Table 4.1. Hydrogen activation in Pt sites could terminate the chain growth reaction in FT synthesis leading to higher amount of CH_4.

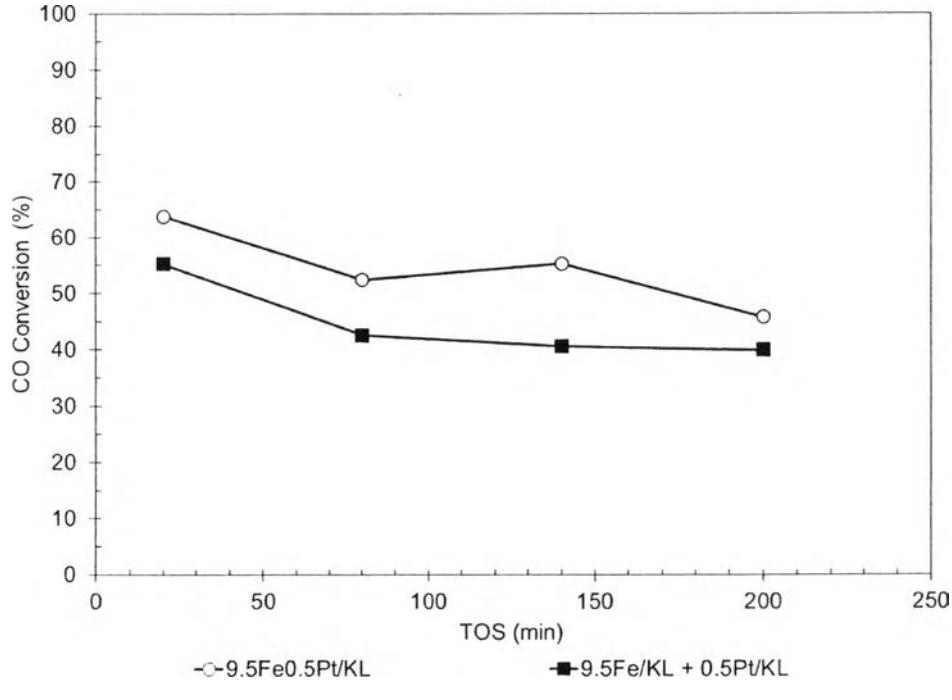

Figure 4.16 CO conversion with time on stream for co-impregnated and physically mixed catalysts (GHSV = 6,000 $cm^3/g.h$, P = 1 atm, T = 400 °C and H_2/CO = 1.5).

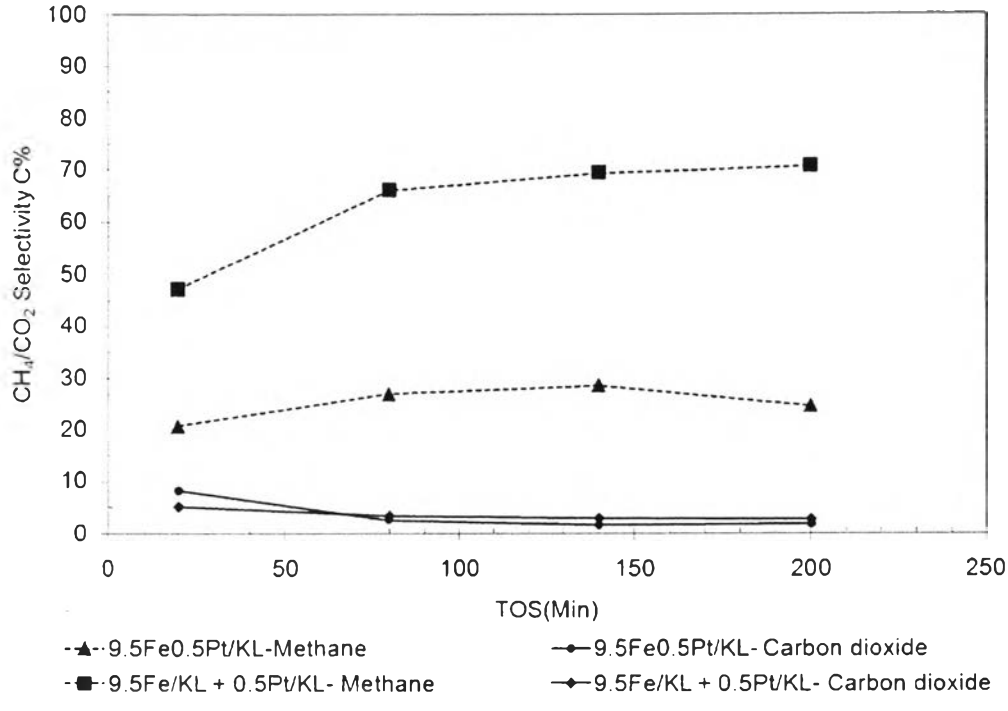

Figure 4.17 CH_4 selectivity with time on stream for co-impregnated and physically mixed catalysts (GHSV = 6,000 $cm^3/g.h$, P = 1 atm, T = 400 °C and H_2/CO = 1.5).

Even though the conversion is slightly lower and selectivity towards low value products is higher for physically mixed catalyst, a significant result can be observed related to the core objective of this work. As it can be observed in Figure 4.18, the aromatic products selectivity is much higher in physically mixed catalysts. Total aromatic selectivity is 7 % at the initial stage but decreased to less than 3 % after 200 min on stream, which is comparatively higher than co-impregnated which shows around 1-2 % selectivity.

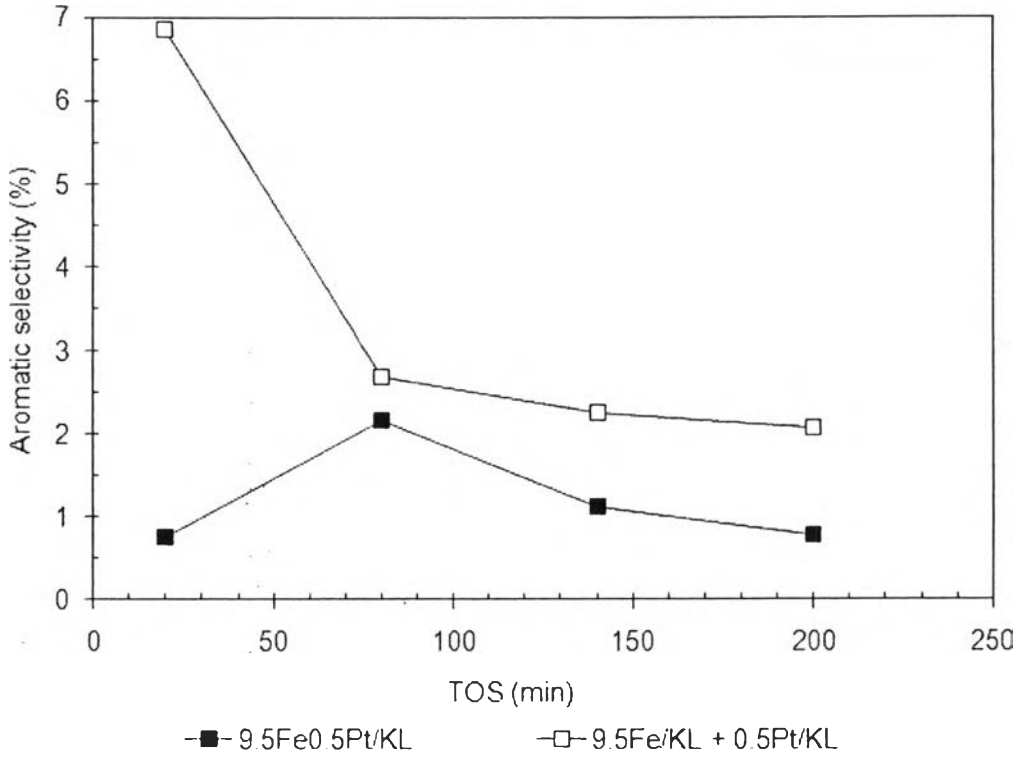

Figure 4.18 Aromatics selectivity with time on stream for co-impregnated and physically mixed catalysts (GHSV = 6,000 $cm^3/g.h$, P = 1 atm, T = 400 °C and $H_2/CO = 1.5$).

These results suggest that the physically mixed catalysts produce more aromatics than co-impregnated catalysts. This result is in line with the observed pore blockage in co-impregnated catalyst leading to poor accessibility to Pt sites inside the pores, which are important for aromatization with Pt/KL catalyst. In BET analysis in Table 4.1, it was observed that a significant pore blockage in 9.5Fe/KL but in the case of 0.5Pt/KL catalysts, accessible Pt inside pore is available. Hence, further analysis will be followed with physically mixed hybrid catalysts.

It is known fact that the heavy product fraction in FT synthesis increases with increasing pressure and hence a test was carried out to observe the influence of the pressure for reaction. A special pretreatment called carbiding was conducted prior to high-pressure run to improve the FT activity of the catalyst. The notation HP/CB is used here to denote that high-pressure operation with carbiding treatment.

It was observed that the conversion has significantly improved with high-pressure operation with carburizing pretreatment as illustrated in Figure 4.19 below. This implies that carbiding pretreatment for catalyst activation is important in improving the FT activity as discussed by Martinez and co-workers (2005). In addition, the total of CO_2 and CH_4 selectivity is relatively high with almost same values around 60-70 % as presented in Figure 4.20 and this is disadvantageous to lose C as low value products.

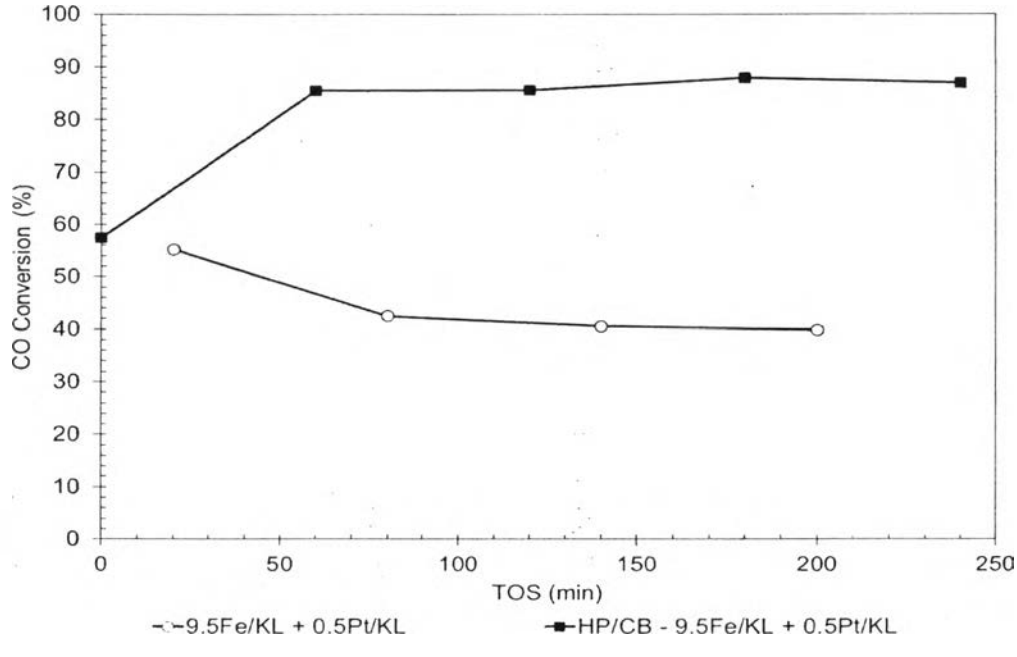

Figure 4.19 Variation of conversion with time on stream of physically mixed Fe/KL and Pt/KL with and without high pressure (HP = 20 bar) conditions and carbiding (CB) treatment (GHSV = 6,000 cm^3/g.h, T = 400 °C and H_2/CO = 1.5).

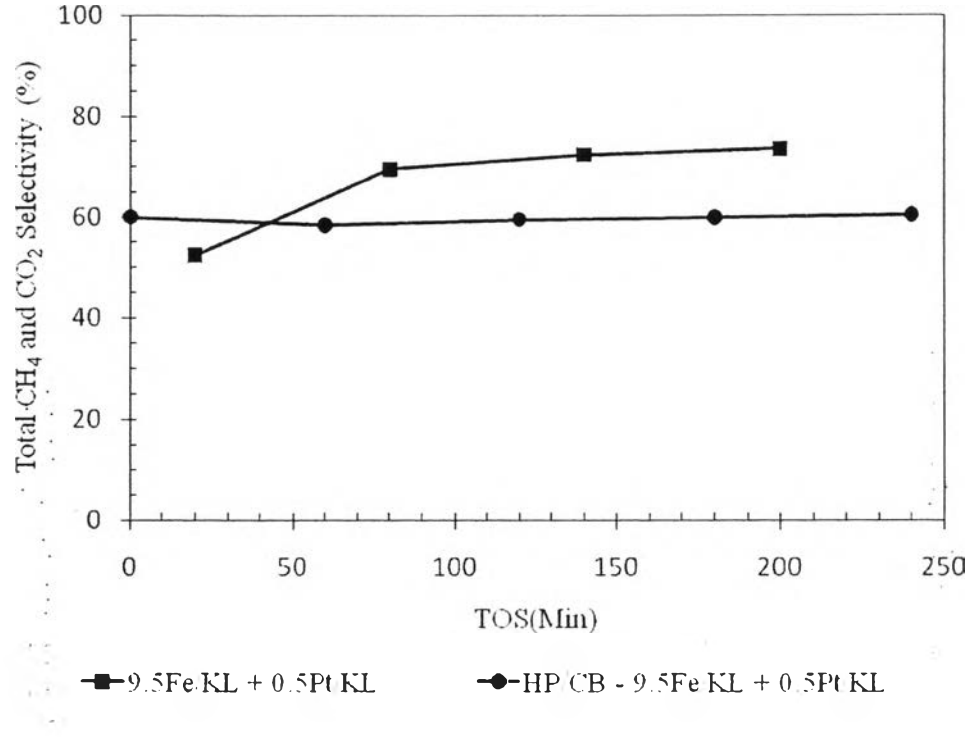

Figure 4.20 Total CO_2 and CH_4 slectivity with time on steam of physically mixed Fe/KL and Pt/KL with and without high pressure (HP = 20 bar) condition and carbiding (CB) treatment (GHSV = 6,000 $cm^3/g.h$, T = 400 °C and H_2/CO = 1.5).

However, aromatics selectivity at high-pressure operation is observed as low as 1%, which is lower than that of atmospheric pressure operation as shown in Figure 4.21. From the results as presented in Figure 4.22, it can be observed that it has a significantly higher amount of C_{3+} fraction including C_6-C_8 hydrocarbon after the aromatization reaction, which was not converted to aromatics. This could be due to the poisoning effect of Pt by CO.

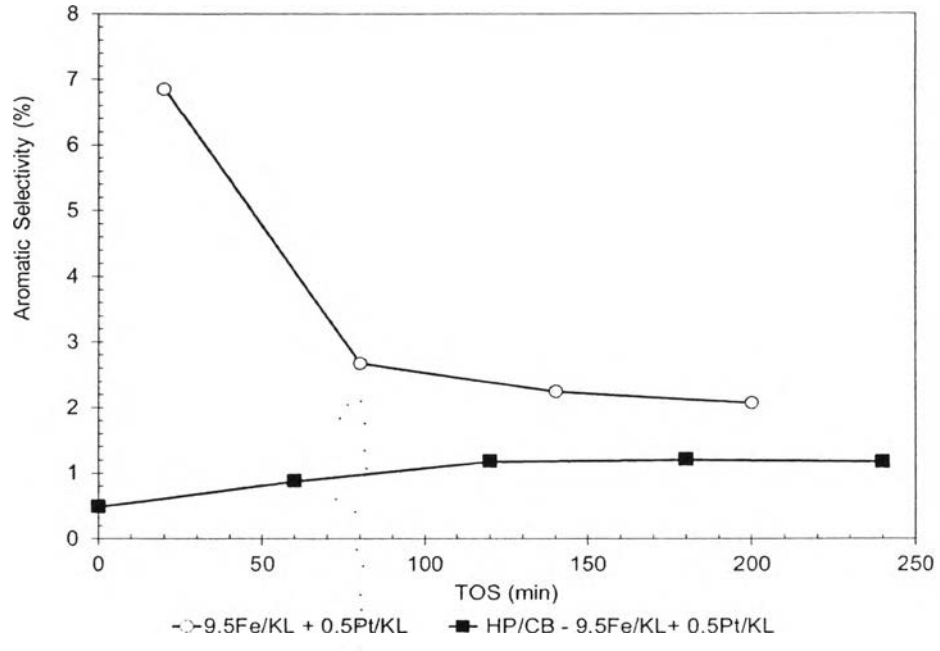

Figure 4.21 Aromatic selectivity with time on stream of physically mixed Fe/KL and Pt/KL with and without high pressure (HP = 20 bar) condition and carbiding (CB) treatment (GHSV = 6,000 $cm^3/g.h$, T = 400 °C and H_2/CO = 1.5).

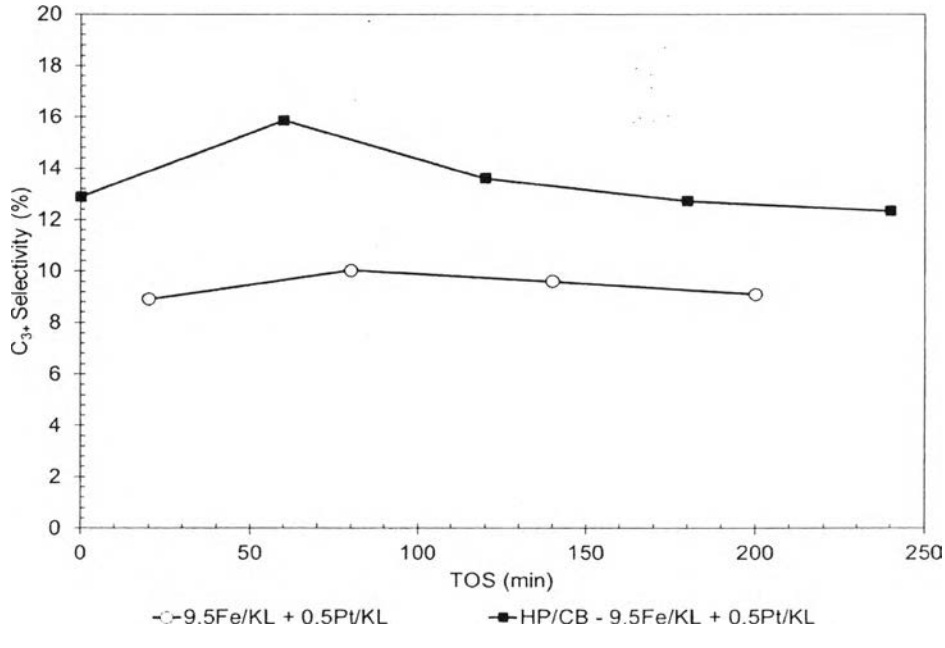

Figure 4.22 C_{3+} fraction selectivity with time on stream of physically mixed Fe/KL and Pt/KL with and without high pressure (HP = 20 bar) condition and carbiding (CB) treatment (GHSV = 6,000 $cm^3/g.h$, T = 400 °C and H_2/CO = 1.5).

In addition, the performance of syngas conversion to aromatics with physically mixed FeCoK and Pt/KL catalysts showed poor aromatic production even though FeCoK can produce higher C_{3+} fraction in FT synthesis compared to 9.5Fe/KL. The aromatic selectivity is negligible even though it has sufficient amount of paraffinic products which supposed to be aromatized with Pt/KL as presented in Figure 4.23.

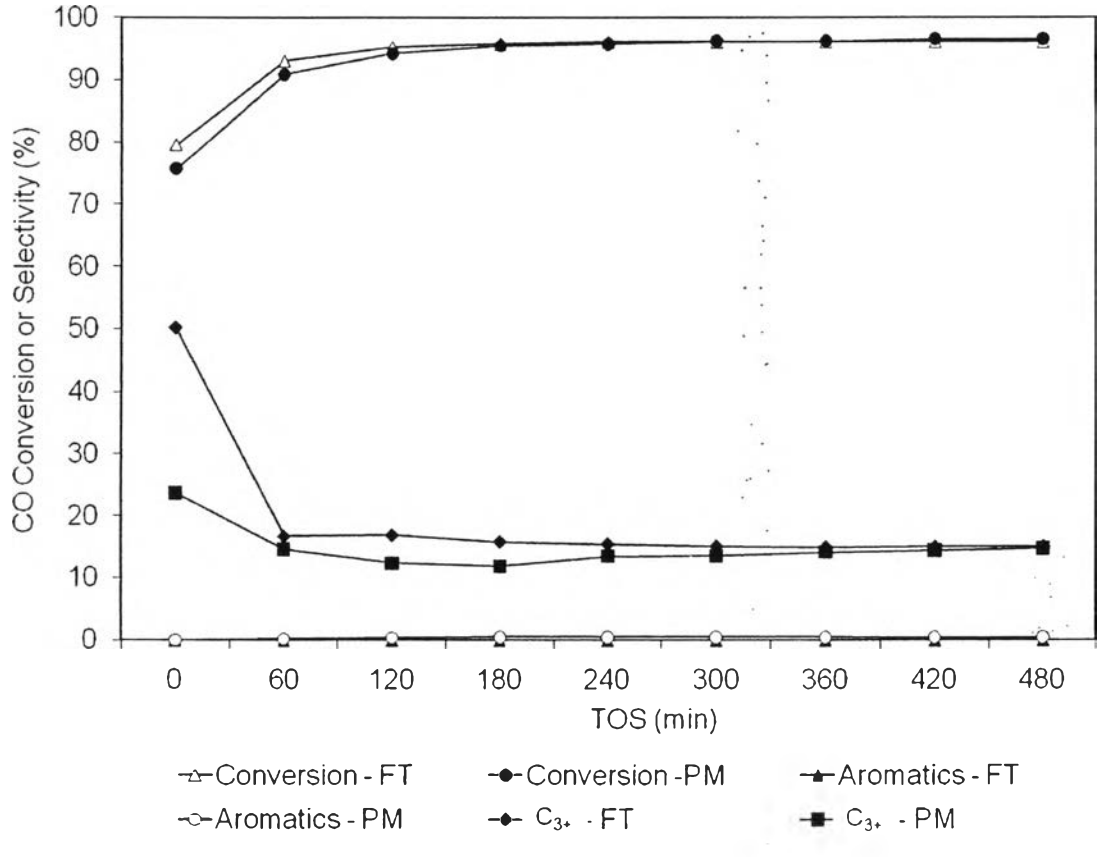

Figure 4.23 Conversion, C_{3+} fraction and aromatics for FeCoK FT catalyst (FT) and physically mixed FeCoK with Pt/KL (PM) with TOS (GHSV = 6,000 $cm^3/g.h$, T = 400 °C, P = 20 bar, and H_2/CO = 1.5).

Total product distribution for tests with different catalysts and different process conditions for syngas aromatization after 200 min TOS are presented in Table 4.7.

Table 4.7 Total product distribution for syngas aromatization reactions with Pt/KL aromatization catalysts (GHSV = 6,000 $cm^3/g.h$, T = 400 °C, and H_2/CO = 1.5)

	9.5Fe0.5Pt/KL	9.5Fe/KL+0.5Pt/KL	HP/CB-9.5Fe/KL+0.5Pt/KL	HP/CB-FeCoK+0.5Pt/KL
CO Conversion	45.78	39.89	86.97	96.06
Non aromatics				
CO_2	3.81	5.46	19.08	31.09
C_1	24.63	70.76	41.30	29.74
C_2	25.40	7.81	15.16	11.66
C_3	35.80	4.79	10.98	12.06
C_4	0.00	4.87	5.60	6.28
C_5	6.18	4.24	3.30	5.30
C_6	3.40	0.00	1.87	2.15
C_7	0.00	0.00	0.91	1.03
C_8	0.00	0.00	0.65	0.71
Aromatics	0.77	2.07	1.21	0.46
Benzene	0.77	0.67	0.24	0.15
Toluene	0.00	1.40	0.63	0.31
Etyl benzene	0.00	0.00	0.08	0.00
Xylenes	0.00	0.00	0.26	0.00
AC_{9+}	0.00	0.00	0.00	0.00

In all the cases, it seems that significant fraction of hydrocarbons produced which supposed to be converted to aromatics is remained unconverted. The suspected reason for unsatisfactory aromatization is poisoning the Pt/KL zeolite catalyst by CO and it seems that after pretreatment of carburizing with CO, aromatic production is lower even though it was observed that Fe could increase the CO tolerance of Pt/C catalysts (Pereira *et al.*, 2009). Hence, an aromatization test was carried out for aromatization of n-hexane with intermittent injection of CO with feed.

In the test with 0.5Pt/KL zeolite to convert n-hexane to aromatics, it was observed that conversion and aromatization showed a significant value as 70% and 60% respectively at 500 °C. A flow of 120 ml of CO was injected in 15 min with n-hexane feed maintaining the same reactor temperature. With that, the conversion decreased drastically along with aromatic production. This indicates that CO retards the function of Pt/KL catalyst for aromatization as presented in Figure 4.24.

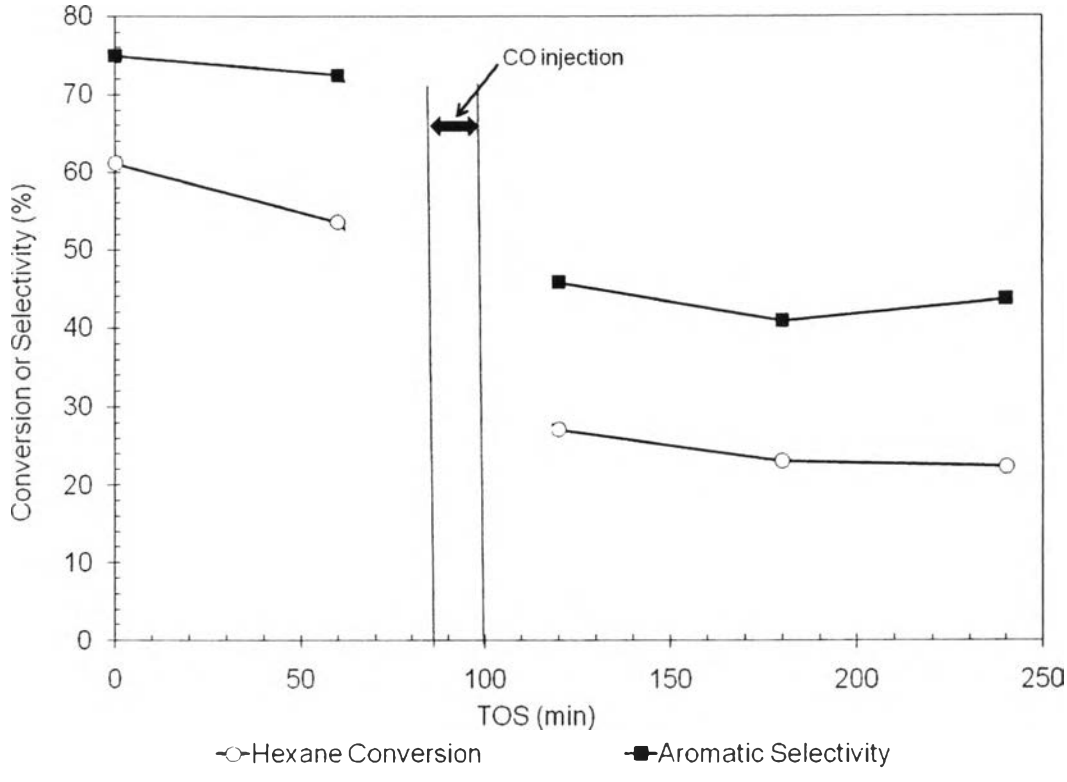

Figure 4.24 Influence of CO on hexane conversion and aromatic selectivity over Pt/KL catalyst (SV= 5 h^{-1} with 0.5 g of catalyst, T= 500 °C, P = 1 atm, H_2/n-hexane = 6).

This result indicates that the 0.5Pt/KL catalyst exhibited high activity and selectivity for aromatization. In addition, the Pt/KL catalyst was quickly deactivated with CO injection and the activity is not recovered even after CO injection period.

These results encourage the idea of exploring ZSM5 for aromatization instead of Pt/KL zeolite with a best available FT catalyst based on previous studies, which have better product selectivity and activity such as FeCoK instead of Fe/KL zeolite.

4.2.3 Syngas Aromatization with Physically Mixed FeCoK Catalyst and HZSM5 (with Different Proportions)

FeCoK catalyst mixed with HZSM5 (Si/Al = 23) was tested for syngas aromatization by varying the portion of each catalyst to observe the influence to activity and selectivity. Si/Al =23 was selected due to sufficient acidity which leads to higher aromatization activity (Martinez *et al.*, 2005).

Commercial ZSM5 in NH_4^+ form, which is in pellet form, was crushed to powdered form followed by calcining at 500 °C for 5 h to form HZSM5. The commercial ZSM5 used contains 20 % of alumina as binder and the portion of HZSM5 in the physical mixture is measured as pure HZSM5 basis.

Tests for the study of aromatization possibility were conducted with varying ratios of HZSM5 to FeCoK with HZSM5 weight percentage of 0 (FeCoK) , 33 (33ZFeCoK), 44 (44ZFeCoK), 67(66ZFeCoK), 75 (75ZFeCoK) and 80 (80ZFeCoK). All the tests were conducted with in situ reduction at 400 °C for 10 h with a heating rate of 1 °C/min followed by cooled down to 100 °C. Carburizing was conducted after reduction, with a mixture of feed with He having $CO:H_2:He$ = 10:15:75 which was conducted at 400 °C for 3 h with a heating rate of 1 °C/min. The reaction was run at 20 bar pressure and 310 °C temperature with a heating rate of 4 °C/min for syngas containing H_2/CO = 1.5.

With the variation of HZSM5 percentage in hybrid catalyst, it is clear that the CO conversion is always as high as 95% and no any significant variation with HZSM5 addition to hybrid catalyst as presented in Figure 4.25. This information indicates that FeCoK mainly governs the conversion of CO in the hybrid catalyst and HZSM5 shows no activity or promotional effect on CO conversion by hybrid catalysts FeCoK with HZSM5 contradicting with the work of Martinez and co-workers on high-octane gasoline production from syngas. The increase in the conversion at the beginning until 130 minutes could be due to the unstable condition in the system due to dilution of reaction products in the reactor downstream. In addition, variation in reactor temperature was observed at early stages of the reaction, hence influence from that too might induce some effect on this instability.

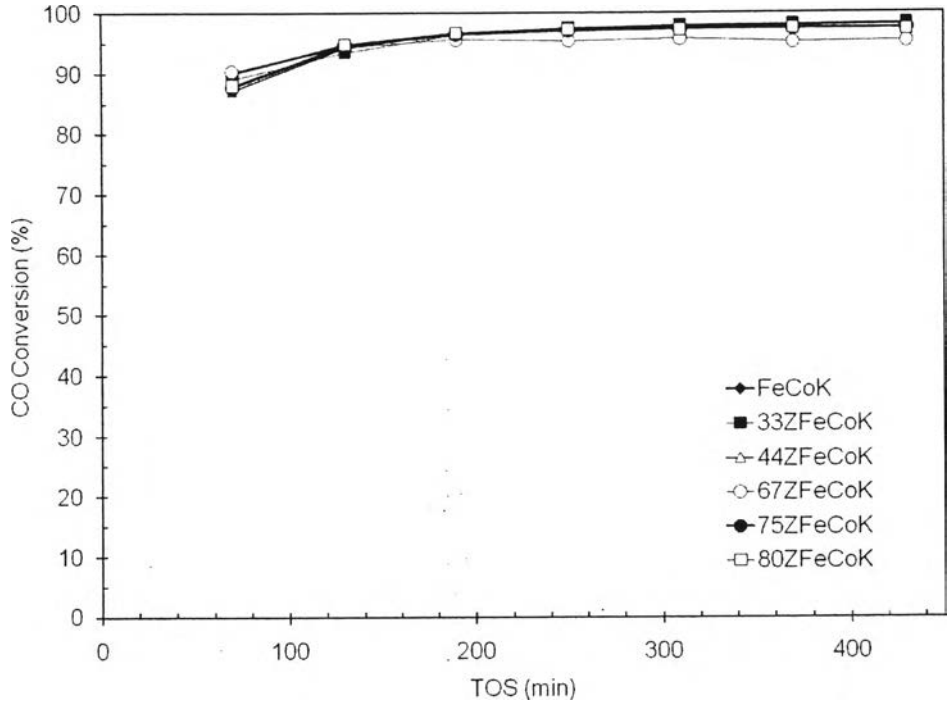

Figure 4.25 CO conversion for hybrid catalysts of FeCoK and HZSM5 with time on stream (GHSV = 4,800 $cm^3/g.h$, T = 310 °C, P = 20 bar, and H_2/CO = 1.5).

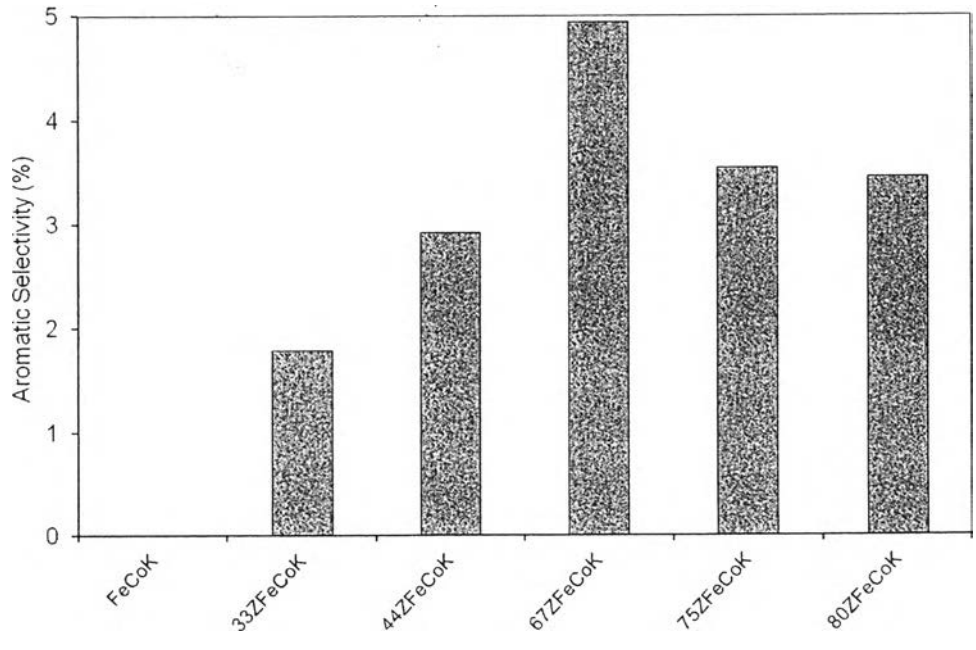

Figure 4.26 Aromatic selectivity for hybrid catalysts of FeCoK and HZSM5 at 430 min TOS (GHSV = 4,800 $cm^3/g.h$, T = 310 °C, P = 20 bar, and H_2/CO = 1.5).

The highest aromatic selectivity is observed as HZSM5 percentage in the hybrid catalyst increased up to 67% and showed a decrease with further increase of HZSM5 percentage as shown in Figure 4.26. This shows that the increase of HZSM5 content in hybrid catalysts beyond 67% is not positively influenced for aromatic production.

Further, as indicated in Figure 4.27, it is observed that aromatic selectivity is increased with increasing TOS for all the hybrid catalysts. The increase in the aromatic selectivity with TOS shows a significant relationship to the product selectivity of FT synthesis with TOS as shown in Figure 4.28. In the FT synthesis with FeCoK catalyst at same conditions shows an increase in C_{5+} fraction (C_5 and above) with TOS and the increase in aromatic selectivity seems related to this increase in C_{5+} fraction. This information suggests that the aromatics formed in hybrid catalysts of FeCoK and HZSM5 are mainly from aromatization of C_{5+} products of FT synthesis. The combined graph is presented in Figure 4.29.

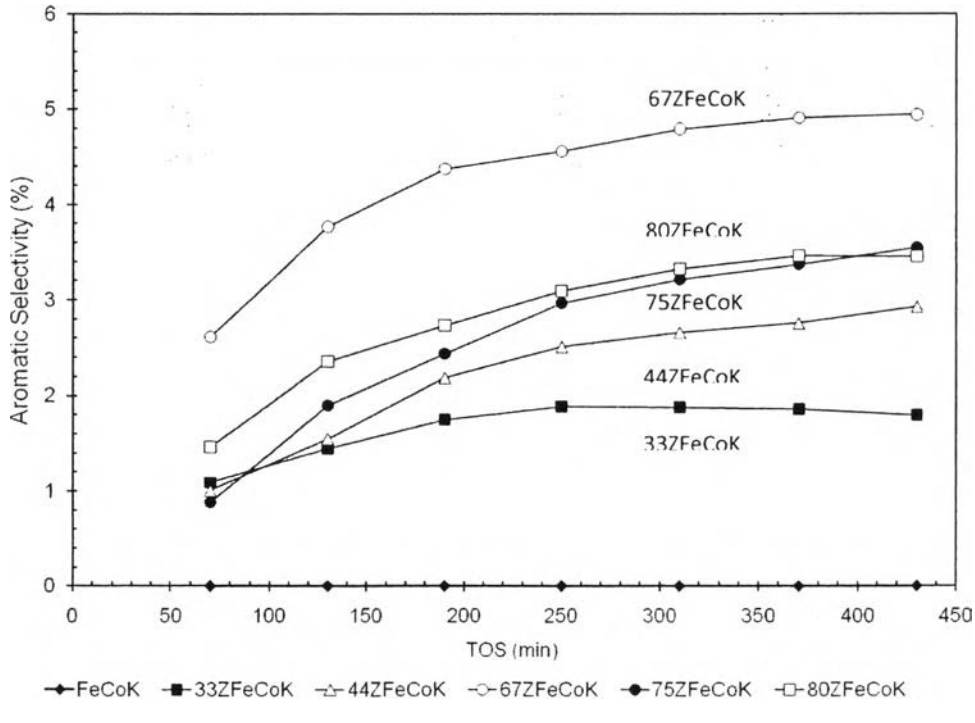

Figure 4.27 Aromatic selectivity for hybrid catalysts of FeCoK and HZSM5 with TOS (GHSV = 4,800 $cm^3/g.h$, T = 310 °C, P = 20 bar, and H_2/CO = 1.5).

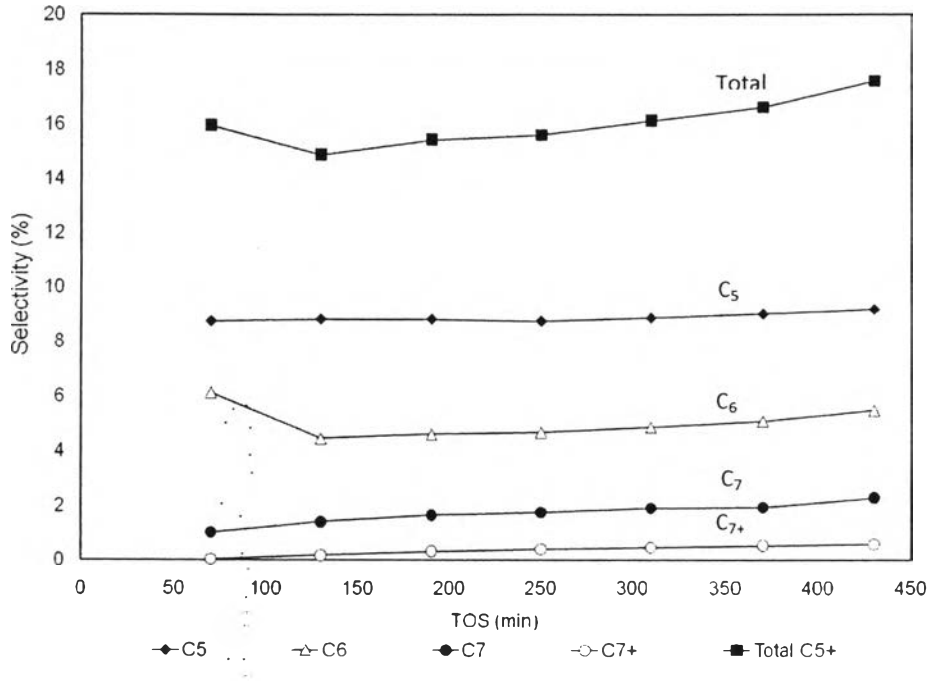

Figure 4.28 Change of C_{5+} product fraction and individual carbon number selectivity for FeCoK catalyst with TOS (GHSV = 4,800 $cm^3/g.h$, T = 310 °C, P = 20 bar, and H_2/CO = 1.5).

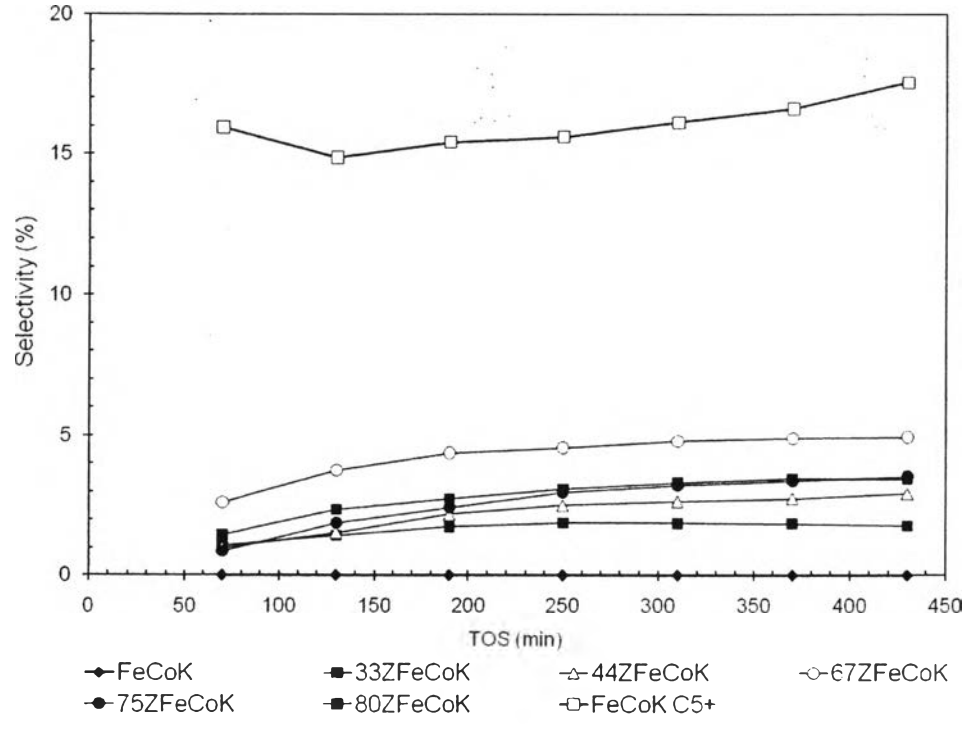

Figure 4.29 Selectivity of C_{5+} for FeCoK and aromatic for hybrid catalysts with TOS (GHSV = 4,800 $cm^3/g.h$, T = 310 °C, P = 20 bar, and H_2/CO = 1.5).

The lower aromatic selectivity is observed for 33ZFeCoK and 44ZFeCoK could be due to the insufficient availability of HZSM5, which governs the aromatization activity.

As HZSM5 plays a role in both aromatization and cracking, the availability of HZSM5 leads to produce aromatic and light products by aromatization and cracking respectively. In the cases of higher contents of HZSM5 in the hybrid catalysts, it is observed that light hydrocarbons are increased as shown in the Figure 4.31. This could be due to the available external surface of HZSM5 for cracking activity. This could be the reason for lower aromatic in the cases of 75 and 85% HZSM5 in the hybrid catalysts.

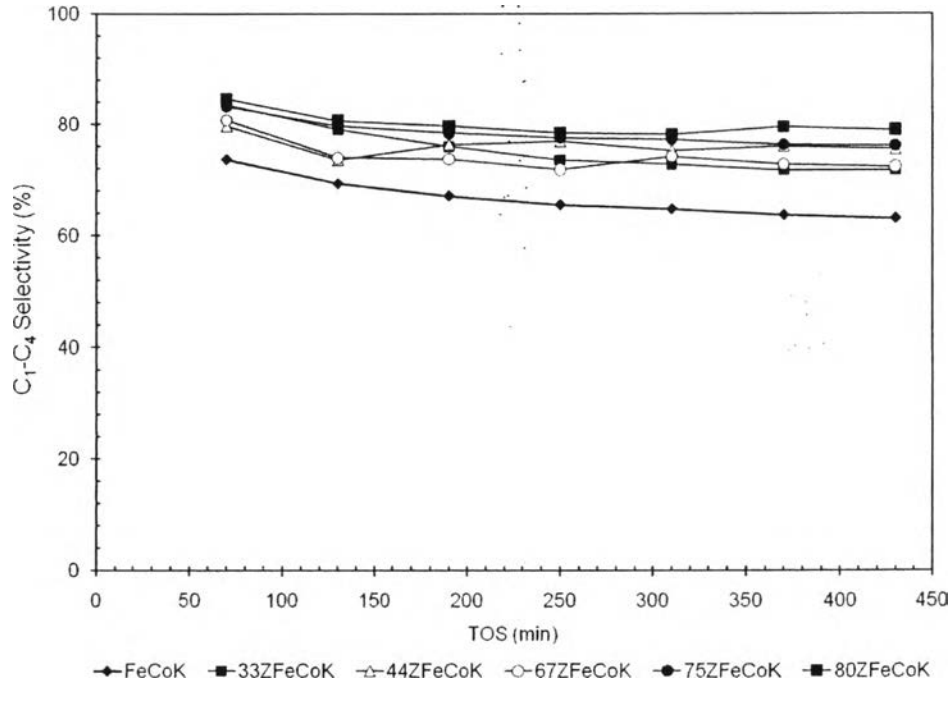

Figure 4.30 Selectivity of C_1-C_4 for FeCoK and hybrid catalysts with TOS (GHSV = 4,800 $cm^3/g.h$, T = 310 °C, P = 20 bar, and H_2/CO = 1.5).

CO conversion and total product distribution in each activity test with hybrid catalysts of FeCoK and HZSM5 is presented in Table 4.8 after 430 min TOS.

Table 4.8 CO conversion and product selectivity for different hybrid catalysts after 430 min TOS (GHSV = 4,800 cm^3/g.h, T = 310 °C, P = 20 bar, and H_2/CO = 1.5)

	FeCoK	33ZFeCoK	44ZFeCoK	67ZFeCoK	75ZFeCoK	80ZFeCoK
CO Conversion	98.03	98.23	97.71	95.30	97.40	97.19
Non aromatics						
CO_2	19.39	20.69	16.00	16.88	18.41	15.86
C_1	20.21	21.16	22.51	25.59	24.69	24.64
C_2	22.01	7.24	6.77	5.88	4.64	4.38
C_3	16.96	12.11	15.46	25.89	27.46	31.09
C_4	3.88	31.22	30.72	15.00	19.30	18.87
C_5	9.18	4.40	4.68	5.28	1.69	1.53
C_6	5.49	1.22	0.88	0.43	0.25	0.18
C_7	2.30	0.16	0.28	0.11	0.02	0.00
C_8	0.59	0.00	0.00	0.00	0.00	0.00
Aromatics	**0.00**	**1.79**	**2.69**	**4.94**	**3.55**	**3.45**
Benzene	0.00	0.39	0.52	1.15	1.32	1.26
Toluene	0.00	1.13	1.37	2.66	1.76	1.74
Ethyl benzene	0.00	0.07	0.17	0.28	0.12	0.11
Xylenes	0.00	0.22	0.63	0.85	0.35	0.35
A_{C9+}	0.00	0.00	0.00	0.00	0.00	0.00

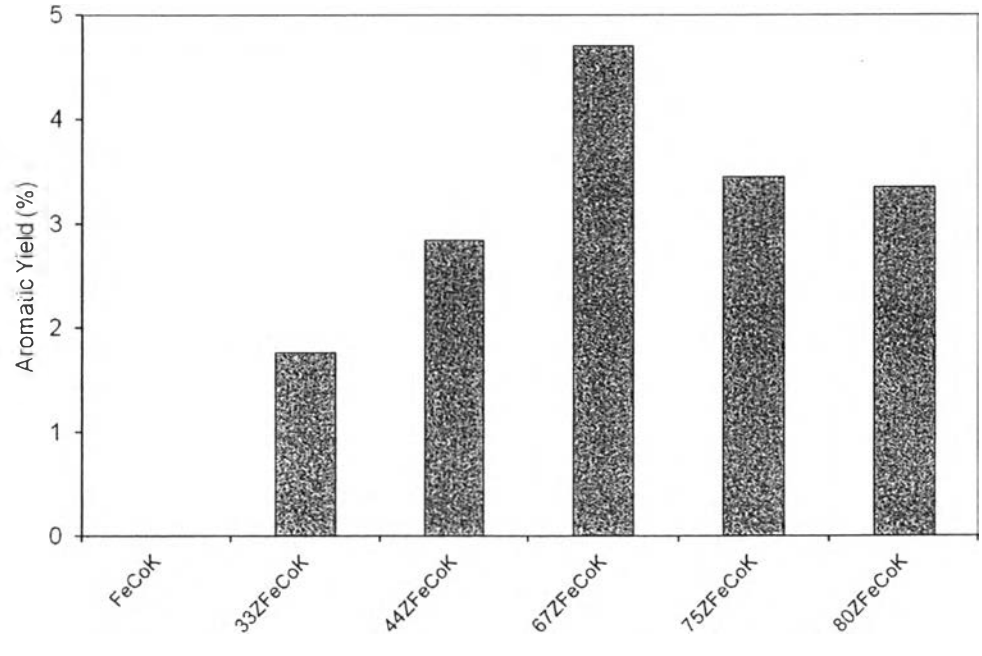

Figure 4.31 Aromatic yield for FeCoK and hybrid catalysts after 430 min TOS (GHSV = 4,800 cm^3/g.h, T = 310 °C, P = 20 bar, and H_2/CO = 1.5).

The highest aromatic yield is obtained with hybrid catalyst 67ZFeCoK at 430 min time on stream because the conversion is not significantly affected by the amount of HZSM5 content in the catalyst showing around 95% for all the cases. Hence the variation of aromatic yield is same as the aromatic selectivity giving highest aromatic yield of 4.7% with 67ZFeCoK after 430 min time on stream as shown in Figure 4.32.

With all above results, it can be observed that availability of sufficient amount of HZSM5 catalyst is very important in converting syngas to aromatics because in the case of 33ZFeCoK and 44ZFeCoK, aromatic yield is low due to insufficiency if HZSM5 catalyst. The higher amount of HZSM5 is also unfavorable for syngas aromatization due to change of product selectivity to lighter products, which are difficult to aromatize with HZSM5 at lower temperatures like 310 °C. The combination of 67ZFeCoK (HZSM5/FeCoK = 2) is observed as best performer providing the highest aromatic selectivity among the combinations studied.